

Claremont Colleges

Scholarship @ Claremont

CGU Theses & Dissertations

CGU Student Scholarship

Fall 2019

Model Predictive Energy Management for Building Microgrids with IoT-based Controllable Loads

Duc Hoai Tran

Claremont Graduate University

Follow this and additional works at: https://scholarship.claremont.edu/cgu_etd



Part of the [Electrical and Computer Engineering Commons](#)

Recommended Citation

Tran, Duc Hoai. (2019). *Model Predictive Energy Management for Building Microgrids with IoT-based Controllable Loads*. CGU Theses & Dissertations, 349. https://scholarship.claremont.edu/cgu_etd/349.

This Open Access Dissertation is brought to you for free and open access by the CGU Student Scholarship at Scholarship @ Claremont. It has been accepted for inclusion in CGU Theses & Dissertations by an authorized administrator of Scholarship @ Claremont. For more information, please contact scholarship@cuc.claremont.edu.

MODEL PREDICTIVE ENERGY MANAGEMENT FOR BUILDING MICROGRIDS
WITH IOT-BASED CONTROLLABLE LOADS

by

Duc Hoai Tran

Claremont Graduate University and California State University Long Beach

2019

© Copyright Duc Hoai Tran, 2019 All rights reserved.

APPROVAL OF THE DISSERTATION COMMITTEE

This dissertation has been duly read, reviewed, and critiqued by the Committee listed below, which hereby approves the manuscript of Duc Hoai Tran as fulfilling the scope and quality requirements for meriting the degree of PhD in Engineering and Industrial Applied Mathematics.

Masoud H. Nazari, Chair
California State University Long Beach
Assistant Professor

Aftab Ahmed
California State University Long Beach
Assistant Professor

Marina Chugunova
Claremont Graduate University
Professor

Ali Nadim
Claremont Graduate University
Professor

ABSTRACT

MODEL PREDICTIVE ENERGY MANAGEMENT FOR BUILDING MICROGRIDS WITH IOT-BASED CONTROLLABLE LOADS

By

Duc Hoai Tran

This thesis develops an economic scheduling framework for a building microgrid with internet of things (IoT) based flexible loads to synchronize the buildings' controllable components, with occupant behavior and environmental conditions. We employ model predictive control (MPC) methods to minimize building operating costs, while maximizing the utilization of the on-site resources. The main research thrusts are: 1) Developing the building microgrid model; 2) Defining different building operation strategies; 3) Minimizing the building's daily operating costs. Simulation results show that the proposed approach provides superior energy cost savings and peak load reduction in comparison with other operation controls, such as All from Utility (AFU), AFU with installed IoT-based Building Energy Management System (BEMS), and MPC-Mix Integer Linear Programming (MILP) without IoT-based BEMS. An economic analysis is also conducted to provide a road map for the implementation of installing advanced energy efficiency technologies across loads in building microgrid and integrating them with the building microgrid's control strategy.

Claremont Graduate University and California State University Long Beach: Fall 2019

ACKNOWLEDGEMENTS

First, I would like to express sincere appreciation to my advisor, Professor Masoud Nazari, Department of Electrical Engineering, California State University Long Beach. Without his kindly assistance and valuable suggestions, this dissertation would not be able to complete and become what it is. Thank you for always showing me your excitement and enthusiasm when teaching and researching. It has highly motivated me during my graduate studies.

In addition, I would like to express grateful to the committee members, Professor Marina Chugunova, Professor Ali Nadim, and Professor Aftab Ahmed, for their constructive comments and valuable evaluations during my proposal presentation and dissertation defense.

Most of all, I am forever thankful to my parents for their endless love, encouragement and support without any conditions.

TABLE OF CONTENTS

	Page
ACKNOWLEDGEMENT	iii
LIST OF TABLES	vi
LIST OF FIGURES	vii
NOMENCLATURE	x
CHAPTER	
1. INTRODUCTION	1
2. FRAMEWORK FOR TRANSFORMING BUILDINGS INTO SMART INFRASTRUCTURES	5
2.1 3-D Model of the Building.....	6
2.2 Data Collection	9
2.3 The IoT Network of the Lighting System and Plug-in Loads	11
2.3.1 IoT network of the lighting system and smart sensors	11
2.3.1.1 Lighting system.....	12
2.3.1.2 Smart sensor system.....	14
2.3.2 IoT network of the plug-in loads	21
2.3.2.1 Optimal placement of smart plug controllers.....	24
2.3.2.2 Model-based optimization protocol	24
2.4 The IoT-based Building Energy Management System (BEMS)	27
3. BUILDING MICROGRID MODELING AND ANALYSIS.....	32
3.1 Distributed Generator Modeling	32
3.2 Energy Storage Modeling	36
3.3 Utility Grid Modeling	42
3.3.1 Peak demand cost modeling.....	43
3.3.2 Energy balancing modeling	43
3.4 PV Power Profile and TOU Rate	44
3.4.1 PV profile.....	44
3.4.2 TOU rate	45
3.5 Forecast Uncertainty Modeling.....	46
4. CONTROL STRATEGY DEVELOPMENT	49
4.1 MILP Principles	50
4.2 Connecting MILP Optimization to Optimal Scheduling	51
4.2.1 Cost objective function	53

CHAPTER	Page
4.2.2 MILP control system.....	53
4.3 The Proposed MPC-MILP Control Approach.....	55
4.3.1 MPC principles	55
4.3.2 MPC-MILP control strategy	55
5. CASE STUDY: SIMULATION AND RESULTS.....	58
5.1 Proposed ECS Building Microgrid.....	58
5.2 Control Strategy Setup.....	61
5.3 Simulation and Results	61
5.4 Unit commitment and Economic Dispatch Discussion	64
5.5 Economic Analysis	65
5.5.1 Benefits from implementing IoT-based BEMS	65
5.5.2 Saving and payback period	67
6. CONCLUSION.....	69
APPENDIX A: Matlab code of the proposed MPC-MILP controller.....	71
APPENDIX B: Simulink Simscape model of ECS microgrid and MPC-MILP controller.....	88
REFERENCES	91

LIST OF TABLES

TABLE	Page
1. Total Number of Lights by Types.....	10
2. Total Number of Outlets by Types	10
3. Plug Loads Inventory	11
4. Inventory of installed smart sensors, gateway, PoE switch, and Energy Manager	17
5. ECS Buildings Plug Load Inventory.....	26
6. Total monthly operational cost, and monthly peak demand comparison ..	64
7. Economic analysis of the proposed project	68

LIST OF FIGURES

FIGURE	Page
1. 3D model of ECS building.....	7
2. Electrical fixtures (lights and plugs) of 5th floor.....	8
3. HVAC system of ECS building.....	8
4. LANCE14 (left) and LANCE24 (right).....	13
5. ILP-SQ4 (left), ILP RZ (middle), and ILP UFO (right).....	13
6. Different types of Enlighted smart sensor (from left to right): a) Micro sensor, b) Surface mount sensor, c) Fixtureless compact sensor.....	15
7. Enlighted smart sensor coverage pattern.....	15
8. Line diagram between Enlighted smart sensor and the Control Unit.....	16
9. Enlighted Energy Manager, Gateway and Control Unit.....	17
10. Floor plan display of lighting fixtures in ECS-411.....	19
11. ECS building occupancy pattern from March 4 to March 10, 2019.....	20
12. Energy consumption of ECS building’s new lighting system for March 2019.....	20
13. Plug load controller layout.....	22
14. Enlighted Plug Load Controller installed at ECS 411.....	23
15. Diagram of Interaction of the Existing EMS, New EMS, and The Enlighted System.....	28
16. Principles of IoT-based BEMS for ECS building.....	30
17. Average space utilization of the ECS building from Jan. 15 to Feb. 15, 2019.....	31

FIGURE	Page
18. Occupancy heat map of the 4 th floor in the ECS building from Jan. 15 to Feb. 15, 2019.....	31
19. The quadratic cost curve (QCC)	33
20. Piecewise linear approximation for the quadratic cost curve	34
21. The QCC and the superimposed linearize segments.....	34
22. Capstone Micro-Turbine C65	36
23. Aspen 48M-25.9 saltwater battery bank	39
24. x^b plot with: 1 battery, 3batteries, 12 batteries.....	40
25. Self-discharge of Aspen 48M-25.9 battery over a month.....	41
26. PV power profile discretized using ZOH.....	44
27. Proposed PV system on the roof of the ECS building	45
28. SCE TOU-8-B purchasing and selling rate	46
29. Forecast modeling method.....	46
30. MILP control system.....	54
31. MPC-MILP control strategy	56
32. Flowchart of microgrid’s operation	56
33. Proposed ECS building microgrid	58
34. PV power forecasting.....	60
35. Demands forecasting.....	60
36. The operation of building microgrid’s components controlled by proposed MPC-MILP approach during May 1 st , 2019	62

FIGURE	Page
37. The operation of building microgrid's components controlled by proposed MPC-MILP approach during May 1 st , 2015	62
38. Operational cost comparison between 4 control strategies for May 2019.....	63
39. DG operation of three examining cases for May 1 st , 2019	65

NOMENCLATURE

x^b	Energy in storage device
x^{Sb}	Energy degradation of storage
D^l	Controllable load's demand
N_{lights}	Number of controllable lighting loads
β^l	Curtailement level of the controllable lighting load
P^b	Power from storage device
x^{DG}	Unit commitment of DG unit
x^{SU}, x^{SD}	Startup/shutdown state of the DG
P^g	Power from the utility grid
c^{peak}	Peak demand cost coefficient
c^{OM}	Operation and maintenance cost coefficient for the DG unit
c^{SU}, c^{SD}	Startup/shut-down cost coefficient for DG
P^{PV}	PV power output
c^P, c^S	Purchasing and selling electricity rates for utility grid [\$/kW]
P^{DG}	Power output from the DG unit
C^{min}	Cost of fuel use for DG at P_{min}^{DG}
s_m, l_m	Slope/power length of segment m
δ^b	Storage charge/discharge decision variables
H_c	Correction time horizon
\hat{P}^{PV}, \hat{D}	PV power, demand forecast prediction
N	Number of equipartition segments

T	Initial prediction horizon length
Z^g	Auxiliary peak demand variable
C^P	Fuel cost from quadratic cost curve
\mathbb{R}	Set of all real numbers
\mathbb{Z}	Set of all real integers
$\{0, 1\}$	Set of all real binary numbers
Δt or T_s	Sampling Period
ε	Machine precision (eps in MATLAB®)
z^b	Supplementary energy storage decision variable
E	User energy consumed
P_{max}^g	Peak Utility Power Requested
OM	Operational and Maintenance Cost Function

CHAPTER 1

INTRODUCTION

A building microgrid, which can represent a commercial, residential, or an industrial building, is a small prosumer (producer-consumer) with local controllers, local consumers, flexible loads, renewable energy resources (RESs), distributed generators (DGs) and/or energy storage devices. The advent of building microgrid technology has opened quality possibilities for electricity market users. For instance, building microgrids increase reliability in power supplied to end users [1]. Moreover, the self-reliance brought on from the utilization of distributed energy resources (DERs) makes this technology attractive for environments where satisfying power demand is critical, such as hospitals, police stations, and emergency operating centers.

Applying advanced energy efficiency technologies across loads in building microgrids is important for energy reduction and increasing demand response capability. For instance, energy efficiency technologies, such as grid-friendly appliances [2]-[4], can be applied across lighting fixtures, plug-in loads, and HVAC systems. Energy efficiency technologies can also use smart sensors, actuators, and microchips [5], [6] to collect and manage data according to buildings functions and services. These advanced sensors and actuators can be connected through an Internet of Things (IoT) platform that enables data collection and data transmission to the Building Energy Management System (BEMS) [7]. The IoT-based BEMS system processes the data and extracts useful information for optimal energy scheduling and facility management, as well as synchronizing the building's energy consumption with environmental conditions, occupant behavior, and power grid operation.

Another aspect of building microgrid management is the optimal scheduling and utilization of on-site resources for cost minimization and energy efficiency improvement [8]-

[12]. Researchers have been studying microgrid configurations, planning, control, and operation strategies because of their benefits to the grid such as increased efficiency, reliability, and resilience. Many algorithms have been proposed for the optimal scheduling of microgrids [13]-[22]. Authors in [13] proposed conventional economic scheduling for the energy management optimization problem by finding a certain set of units (voltages, currents) to satisfy the load. Lagrangian relaxation [14] along with genetic algorithm approach [15], or agent-based modeling and robust optimization [16] have been used for optimal schedule of microgrid. However, the uncertainties of RESs and demand profile have been treated as deterministic data in these studies, which is not always accurate and realistic.

Authors in [19] and [20] presented a mixed integer linear programming (MILP) control strategy, which consider uncertainties of RESs and demand profile as stochastic data, to minimize the operating cost of residential microgrids. The MILP performance, however, could lead to sub-optimal results since decision variables are chosen based on solely the day-ahead forecasts, and they are not updated by the near real-time predictions of the building microgrid states. Authors in [21] and [22] have proposed Model Predictive Control (MPC) in conjunction with MILP optimization (MPC-MILP) to reduce the effects that uncertainty has on operational performance. They proposed updating the forecasts of RESs and demand profile with new data from the microgrid, recalculating the optimal schedule to correct for errors, implementing the control decisions, and repeating the process at fixed time intervals throughout the day.

The main contribution of this research is the employment of MPC-MILP with near real-time prediction horizon (15 minutes time interval) to a real-world building microgrid with a diverse set of on-site resources, such as IoT-based flexible loads, including an IoT network of the lighting system and plug-in loads, distributed solar generation, micro-gas turbine, and energy

storage. The proposed building microgrid is the Engineering and Computer Science (ECS) building at California State University, Long Beach (CSULB). The building has more than 100,000 square feet of conditioned space and through an on-going California Energy Commission (EPC-16- 033) project, it has been equipped with a network of IoT sensors and actuators across the lighting, plug-in loads, and HVAC system.

Specifically, this research develops an MPC-based energy management system with load controllability for the CSULB-ECS building microgrid to minimize daily operating costs. The building operating costs under the proposed MPC-MILP control approach is compared with three scenarios: 1) Purchasing all electricity from the utility grid; 2) The MPC-MILP algorithm (updating forecasts every 15 minutes, but considering all loads as critical loads, and there is no IoT network of sensors and actuator); and, 3) Purchasing all electricity from the utility grid, but with IoT network of sensors and actuators installed. The simulation results show that the proposed MPC-MILP approach with load controllability provides extra saving on the building's operating costs and peak load costs.

This thesis is organized as follows: chapter 2 will provide a framework for transforming building into smart infrastructure and introduce the IoT network of lighting system and plug-in loads. This chapter also addresses one aspect of the smart building design, namely optimal placement of smart sensors and actuators. Chapter 3 will explain the modeling process of the microgrid's components, as well as demand and PV profile. The chapter also introduces the new IoT BEMS of the ECS building. Chapter 4 formulate the MPC-MILP control strategy, and presents the implementation of load controllability, curtailment level constraints and curtailment penalty in the modeling and optimization of the building microgrid. In chapter 5, the MPC-MILP control approach is demonstrated and compared to different operation strategies. The economic

analysis also is conducted in this chapter. Chapter 6 concludes the thesis and provides future research outlook.

CHAPTER 2

FRAMEWORK FOR TRANSFORMING BUILDINGS INTO SMART INFRASTRUCTURES

The combination of residential and commercial buildings account for approximately 40% of the annual energy consumption in the United States [23], and similar statistics apply worldwide [24]. Thus, improving energy efficiency and reducing peak load in buildings opens a door for significant energy savings and cost reduction. There are several opportunities in this area. For instance, up to 40% of energy used by heating, ventilation, and air conditioning (HVAC) systems in commercial buildings is wasted due to faulty operation [25]. Increasing utilization of distributed energy resources (DERs) such as wind turbine and photovoltaics to reduce the dissipated energy by long-distance transmission lines is another opportunity.

Both consumers and utilities can benefit from implementing buildings energy efficient measures. For instance, consumers benefit from reducing energy bills as well as having a more reliable electricity supply. Meanwhile, the deployment of energy efficiency technologies can directly reduce overall and peak hour energy consumption (kWh) and energy demand (kW) from the grid [26].

Typical existing building communication and control flow lack integration of system components and require segregated systems. This results in the challenge of integrating existing products from various vendors. Furthermore, many existing building owners are reluctant to take on brand-new technologies or upgrades due to the need for additional in-house technical personnel and expertise.

Overcoming this reluctance is sought by developing a design process for turning CSULB-ECS building into a smart infrastructure. The building will be smart in the way its electrical

equipment is controlled and eventually will be automated. The tangible objective of work is to examine the opportunities of energy reduction in the CSULB-ECS building in hoping for finding a smart role model for entire campus and beyond.

The analysis in this section is based on the results in the first phase of a three-year smart building design and demonstration project at CSULB, with support from the California Energy Commission (CEC). The goal of this analysis is to remove the barriers to achieve widespread deployment of state-of-the-art energy management technologies in academic buildings by addressing the specific energy needs of such buildings. Particularly, this work will provide California IOUs, academic institutions (i.e. universities including the other 22 CSU campuses), energy management technology developers, and other stakeholders with a detailed customized course of action, an innovative and ubiquitous energy management platform, and comprehensive assessments and documentations of the feasibility of large-scale deployment, technical considerations, performance, savings, and other benefits.

In this regard, the main contribution of this section is developing a framework for transforming buildings into smart infrastructure with high energy efficiency objectives and demand response capability. To such aim, we define and perform the three steps below:

- Specifying load characteristics and operation requirements.
- Identifying loads and devices that can participate in demand response events.
- Developing model-based optimization protocol for smart plug placement.

2.1 3-D Model of The Building

In this sub-section, the 3-D model of the CSULB-ECS building, Figure 1, is developed using Autodesk Revit software [27]. The primary purpose of creating the 3-D model is to identify the optimal location of smart lighting fixtures and plug load controllers. Expected energy

use of the ECS building can be simulated by Revit built-in energy analysis tools. Energy analysis results such as building performance factors, monthly and annual energy use/cost, renewable energy potential will be a useful way to track the effectiveness of building design strategies and energy efficiency measures.

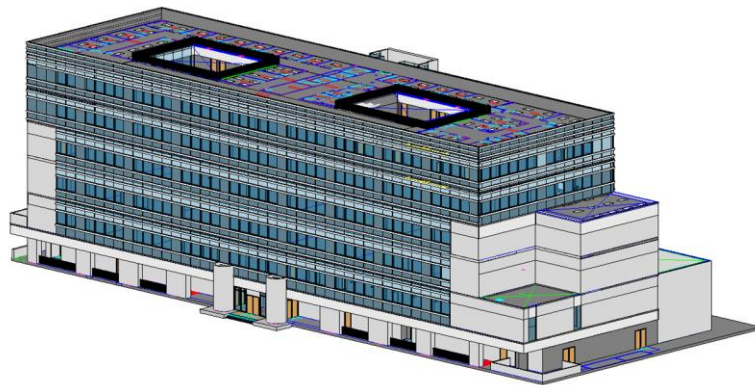


FIGURE 1. 3D model of ECS building

This model was created based on the as-built architectural, structural, and mechanical plans obtained from the Physical Planning and Facilities Management (PPFM) at CSULB. Based on the ECSs architecture plan, the buildings structure was developed with the exact number of measurements such as: walls/ceilings' height and thickness, floors' thickness, columns' dimension, beams dimension. Electrical and mechanical plans were used for creating the 3-D model of the electrical and HVAC systems of the building. This 3-D model is essential for designing the smart building and identifying the optimal location and optimal number of advanced sensors and actuators. Figure 2 shows the electrical fixtures, including lights and plugs, of the 5th floor.

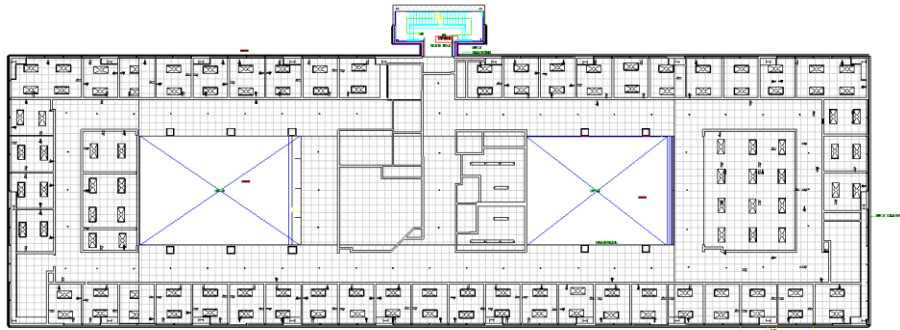


FIGURE 2. Electrical fixtures (lights and plugs) of 5th floor

The HVAC system is simulated and shown in Figure 3. The exterior of the ECS building has been blurred so that the HVAC system, placed inside ceilings, can be seen. The blue pipes in Figure 3 are the duct system with air handlings and air terminals. The size and dimension of the equipment are based on the original mechanical plan.

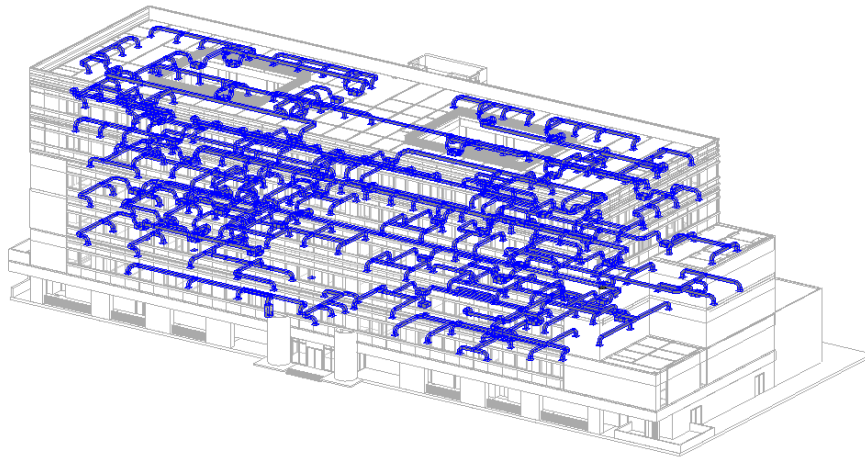


FIGURE 3. HVAC system of ECS building

We conducted two surveys to determine the number of lighting fixtures and outlets in the building. First, we used an exhaustive search by visiting every room in the building to determine the total number of different lighting fixtures and plug loads. Another survey was conducted to

determine the electrical equipment inventory. Accordingly, we obtained a comprehensive load inventory for the building through both 3-D modeling and data collection, as we explain next.

2.2 Data Collection

The comprehensive inventory data in this sub-section helped in estimating the total number of lighting fixtures and plugs, which will be replaced by smart lights and plugs controllers.

The lighting fixtures are classified in four categories: 1) T8 4 Fluorescent (2 or 3 lamps per light fixture); 2) LED; 3) High Intensity Diffusion (HID); and, 4) Halogen lights. The building has a total of 1288 fixtures, and 86% (1119) of all fixtures are fluorescent. There are 2 types of fluorescent fixtures: one type with 2 lamps at 59 watts per fixture, and the second type uses 3 lamps at 89 watts per fixture.

There are also four types of outlets: Single, Duplex, Triplex, and Power Strips. The building has a total of 2522 outlets, and 68% (1702) of them are power strip plugs that mainly power stationary computers and laptops.

Table 1 and 2 illustrate the total number and rated power of lighting fixtures and plugs in the ECS building, respectively. Based on the electrical plan from PPFM, the wattage of outlets is not classified by their types since they are connected to different electrical panels providing different wattages. Hence, table 2 only reports the maximum wattage of each type.

TABLE I. Total Number of Lights by Types

Types of Lights	Florescent Light (2/3 lamps per fixture)	LED	High Intensity Diffusion (HID)	Halogen	Total
Wattage (W)	59/89	12	190	60	
Count	1119	139	18	12	1288

A comprehensive plug load equipment inventory was also conducted to determine different types of plug loads in the ECS building. The plug loads fall into 6 categories as shown in Table 3.

TABLE II. Total Number of Outlets by Types

Types of Outlets	Single	Duplex	Power Strip Plugs	Triplex	Total
Wattage (W)	3220	5000	1280	5000	
Count	4	761	1702	55	2522

There is also specialized equipment, such as fume hood, milling machine, welder, radial saw, planer, and airplane simulator in the dry and wet laboratories.

TABLE III. Plug Loads Inventory

Category	Equipment Type	Total Count	Wattage (W)
Audio/Video	Overhead Projector	31	365
	TV/LCD Screen	28	150
Computers, Monitors	Personal Computer	559	165
	Network Switch	1	66
Gym, Training Equipment	Treadmill	1	700
Kitchen/ Break Room	Refrigerator	11	140
	Coffee Maker	5	936
	Microwave	8	1200
	Water Cooler/ Heater	4	602
	Toaster	3	1500
Lab Equipment	3D printer	9	50
	Oscilloscope/Function Generator/DC Supply	33	50
	Projector Control Unit	1	47
	Personal Printer	112	190
Printer/Scanner	Small Networked Printer	6	567
	Larger Networked Copier/Printer	5	1500
	Fax Machine	2	420
	Paper Shredder	3	146

2.3 IoT Network of The Lighting System and Plug-in Loads

This section will briefly introduce the types and specifications of Enlighted light and Enlighted smart sensor, and Enlighted smart plug controller which have been installed in the ECS building.

2.3.1 IoT network of lighting system and smart sensors

The old lighting system of ECS building does not interface with a controller of network manager. It is not automated even though it has motion sensors that will turn on or off the lights of a room by detecting people's movement.

As mentioned previously, most of the lighting fixtures in ECS building will be replaced by LED lights equipped with smart sensors. The change to LED lights will help reduce the energy consumption of ECS building's lighting system. The sensor attached in each light will allow control and monitoring using IoT technology and will enable near real time demand response.

2.3.1.1 Lighting system

The implementation of the new lighting system has been done by retrofitting lighting fixtures, replacing fluorescent lamps and ballast with LED tubes and control drivers, installing smart sensor at each lighting fixture, and replacing existing wall switches with Enlighted room control switch.

Enlighted IoT architecture consists of a network of LED lights and the smart sensors connected to form the sensor and analytics platform. Data is collected 65 times/second to detect environmental and occupancy changes and act on lighting. Using the IoT based system, it is expected to have the following savings methods:

- Improves overall light quality with LED and sensor light fixtures
- Increases energy savings up to 90%
- Lowers lighting maintenance costs up to 25%
- Collects large volume of data for lighting and other applications
- Task tuning, occupancy data and daylight harvesting increase savings
- Initial installation and services paid for out of energy cost savings
- Unlimited scalability for the enterprise

Different types of LED lights have been installed in the ECS building, including: ILP LANCE 2' X 4' & LANCE 1' X 4', ILP SQ4, ILP RZ4A-30W and RZ8C-60W, ILP UFO low bay. Figure 4 and Figure 5 show these types of lights installed in the ECS building.



FIGURE 4: LANCE14 (left) and LANCE24 (right)



FIGURE 5: ILP-SQ4 (left), ILP RZ (right), and ILP UFO (bottom)

2.3.1.2 Smart sensor system

Each Enlighted smart sensor is a complete sensing and lighting control node powered from its attached light fixture. It captures data that is processed locally and transmitted over the Enlighted network, enabling a full suite of applications. With integrated wireless communications for data transmission and remote configuration as well as autonomous fixture-level control, this sensor brings advanced lighting automation to a whole new level.

Features and benefits:

- Enlighted sensor interface: provides access to device information, energy consumption, and digital lighting control.
- Localized control: communicating wirelessly the light-level schedules, preferences, and behavior profiles for each fixture.
- Field replaceable: allows toolless replacement of the sensors without disturbing the lighting fixture or ceiling tile.
- Smart sensing: supports advanced sensing and detection algorithms, enables optimization of existing features and new future applications.
- Bluetooth low energy: allows the sensor to receive and transmit beacons.
- Occupancy and thermal sensing: A PIR sensor combined with separated ambient and temperature sensing support precise motion identification.
- Tunable white: support configurable lighting transitions based on time of day or user control.
- Daylight harvesting: captured ambient light information is locally processed to raise and lower light levels based on available daylight.

- Room and zone control: pairs with room control switches for code-compliant manual-on/auto-off capability.
- Data reporting: records information regarding occupancy, power consumption, ambient light level, and temperature.

The types of Enlighted sensor that have been used is shown in Figure 6 [26], and sensor coverage pattern is shown in Figure 7.



FIGURE 6: Different types of Enlighted smart sensor (from left to right): a) Micro sensor, b) Surface mount sensor, c) Fixtureless compact sensor

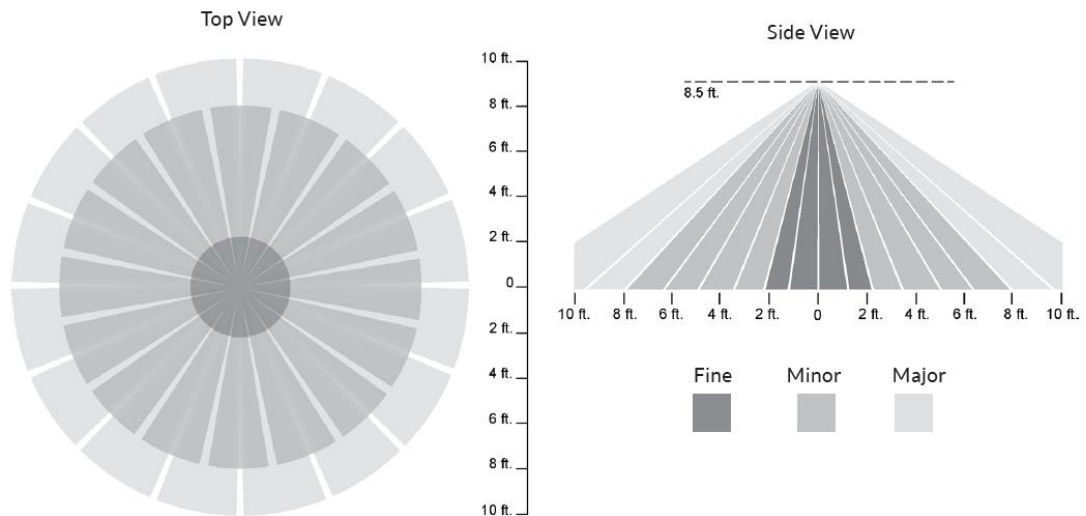


FIGURE 7: Enlighted smart sensor coverage pattern [28]

The smart sensor is designed to be easily mounted into lighting fixtures or ceiling tiles such that only the discrete white faceplate is visible. The sensor slides into a carrier sleeves compatible with lighting fixtures. Each sensor is connected to an Enlighted Control Unit (CU-3E-1R) via 30'' or 12'' CAT3 cable. The control unit rating is 540W @120VAC and 1.246KW @277VAC. Both the compact sensor and the control unit are integrated into each fixture by the fixture manufacturer. The connection layout between the Control Unit and the sensor is shown in Figure 8.

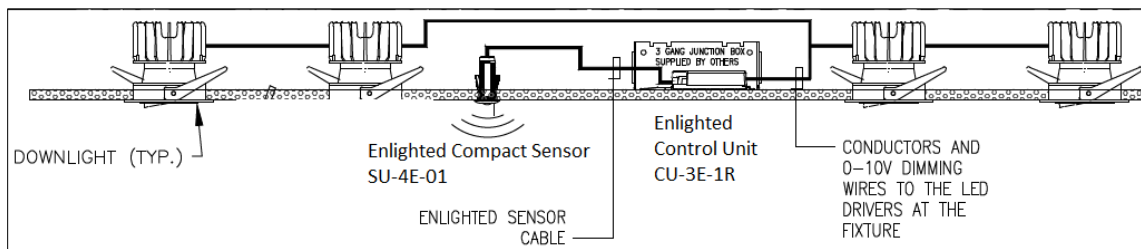


FIGURE 8: Line diagram between Enlighted smart sensor and the Control Unit

Control unit interfaces with the smart sensor and connects to a ballast or LED driver to control light behavior, or receptacle relays to provide on/off controls. The control unit also contains a power metering chip that enables the control network to measure power in real time as well as energy consumption over time.

One or more Gateways may be deployed on each floor to relay information between the sensors and the Enlighted Energy Manager. The Gateway device mounts to the ceiling at the same height as an individual sensor device. The antenna is then pointed down. CAT5e cable is run from the Enlighted Gateway to the Enlighted PoE switch. The PoE switch, sourced from Netgear and certified by Enlighted, powers Enlighted gateway and provides data switching power for Enlighted control network. The control network layout is shown in Figure 9. The number of installed equipment such as smart sensor, POE switch, gateway, etc, is recorded in Table 4.

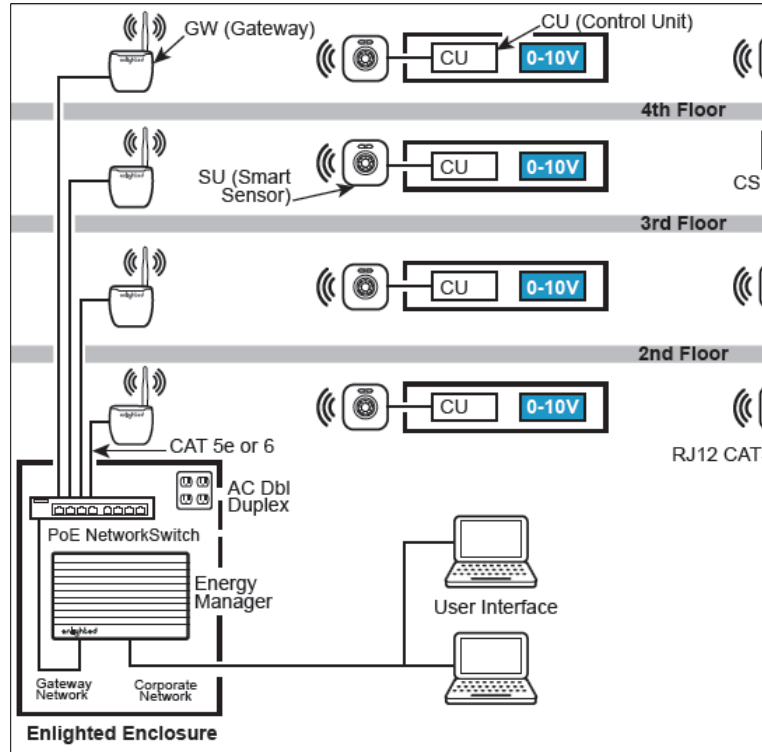


FIGURE 9: Enlighted Energy Manager, Gateway and Control Unit [28]

TABLE 4: Inventory of installed smart sensors, gateway, PoE switch, and Energy Manager

Product Code	Part Number	Description	Quantity
SU-5E-01	01-01961-XX	Enlighted – Kona Embedded Sensor	1023
CU-3E-1R	01-00405-XX	Enlighted - Control Unit - 1% extra included	19
WS-2-00	01-01034-XX	Enlighted - Wireless Room Control (ERC)	155
SU-4S-H	01-01616-XX	Enlighted - Sensor Unit (High Bay) - w/BlueTooth - 1% extra included	19
CBL-2-7F	12-00028-02	Plenum Rated Cable - 7 ft. - for SU2 - 1% extra included	19
BRKT-SU-2-00	11-00057-01	Gen 2 - Sensor Bracket Mount - 8.875" Flat Metal	58
CU-4E-FM	01-02296-03	Enlighted - Fixture Mount Control Unit - for SU5 - 1% extra included	1023

CBL-5E-CU4-30N	12-02290-01	Enlighted - Sensor Cable - 30 In - for SU5 - 1% extra included	1023
WING-CS-D2	05-01315-01	Enlighted - Wing Nut for tile mount sensor - Plastic - (Bag of 100)	1
CS-D2-FL	01-02210-01	Enlighted - 2-Wire Tile Mount Sensor (Sensor Grid Only) - 1% extra included	7
GW-2-01	01-00671-XX	Enlighted - Gateway V2	15
SW-POE-8-8	18-01918-01	8 Port, Managed, PoE Network Gigabit Switch	2
AT-4G-00	06-00540-01	Modem, Wireless, Rugged AL. Casing, 1Eth, 1 USB, 1 RS-232 ports	1
ENCL-EM/FAN	40-00420-02	NEMA 1 Enclosure - w/Fan - for Energy Manager and POE switches	1
EM-2-02	01-01453-XX	Enlighted - Energy Manager - Base sensors = 1,000	1
EM-SW-1	90-01906-01	Per Sensor License	36
PWR-NF	01-02511-01	Enlighted - Power Supply for Sensor Grid Sensors, Max (20) CS-D2-FL sensors, daisy chained	1
FSC-85-RFK-48-132-NB-W-RS	05-00776-01	1x4 1L Strip retrofit Kit (Kit Only & Un-shunted sockets/No Ballast-No pre-wire)	2

Information such as light level, fixture name, fixture MAC, fixture ID, fixture area, fixture profile, fixture type can be accessed through the Enlighted Energy Manager GUI website, Figure 10. The green box in Figure 10 displays the status of the middle lighting fixture in the first line. This lighting fixture is in the auto mode, which varies the light level of the luminaire using sensor input, time of day, day of the week, and values from its operational configuration. The fixture was operating at 55% light level, consuming 22W at the time it has been checked. There is also information regarding occupancy and ambient temperature in the room. The status shown in the fixture icon is updated periodically every 5 minutes.

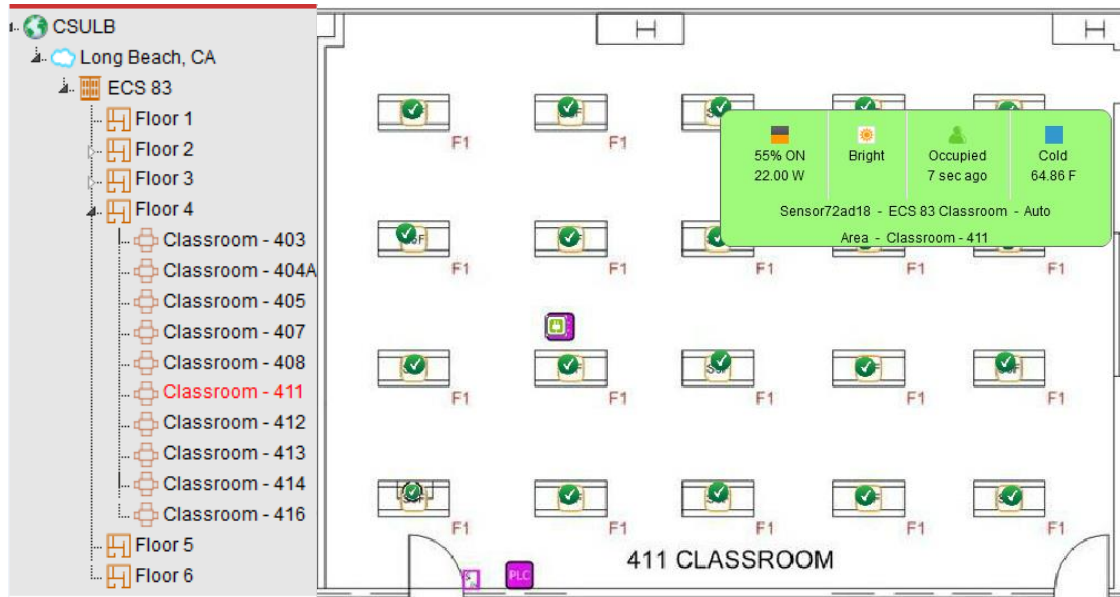


FIGURE 10: Floor plan display of lighting fixtures in ECS-411 [32]

Information collected from each sensor will provide high granularity occupancy information, such as occupancy profiles, space utilization, average occupied hours for different zones, different floors, and the entire building. Figure 11 shows the occupancy profile of the ECS building for one week in March 2019 (March 4 to March 10, 2019), with building business hours being from 7AM to 7PM. As shown in the figure, at 2PM on March 6, on average only 42.79% of the building's zones are occupied and the peak is 46.54%. This important information from the IoT network of sensors provides accurate insight into the building's usage, such as detailed non-intrusive occupancy views, and/or energy usage patterns, which are essential for the energy efficiency and DR algorithms.

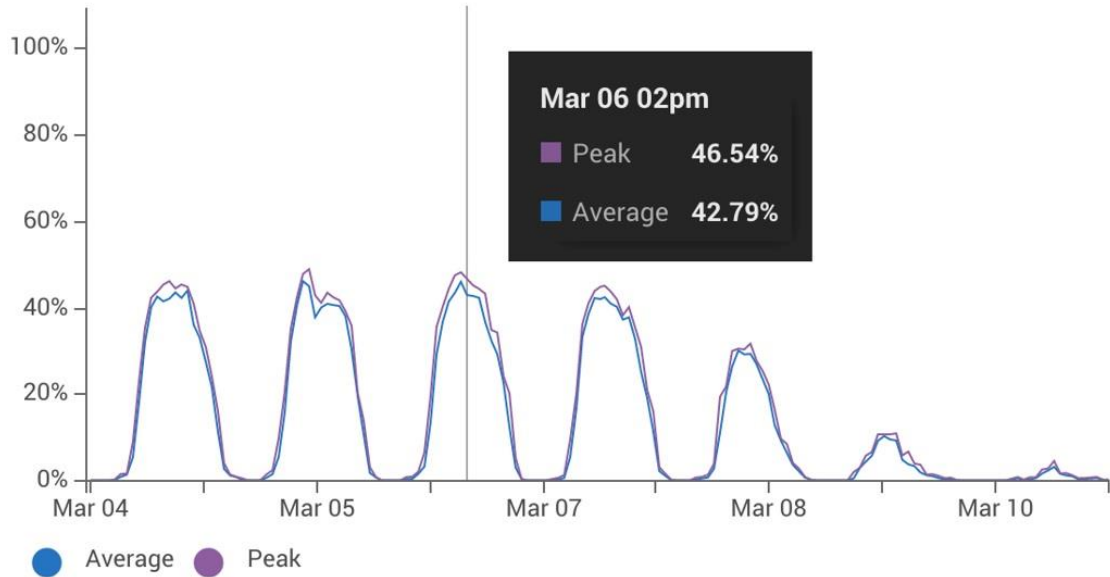


FIGURE 11: ECS building occupancy pattern from March 4 to March 10, 2019 [32].

The Enlighted Energy Manager GUI website also provides the total electricity consumption of the lighting system in different time frames such as day, week, month or year (either for the whole building or desired zone). Figure 12 shows the total energy consumption of ECS building for March 2019, which is 7.13 MWh. The occupancy saving during this period is 10.72 MWh, the daylight harvesting is 181.68 kWh, the task tuning saving is 40.15 MWh. The yielded total saving for this period is 51.05 MWh.

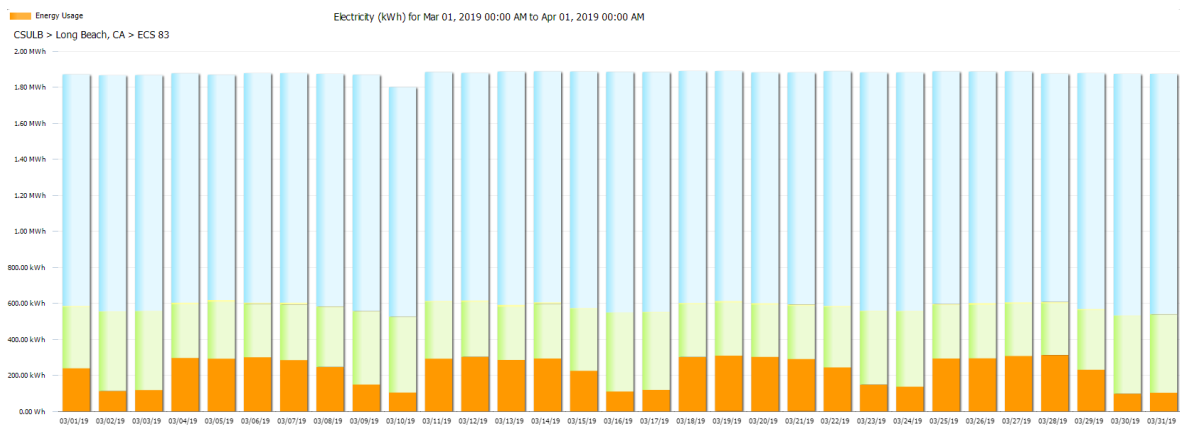


FIGURE 12: Energy consumption of ECS building's new lighting system for March 2019

[32].

The ECS building's smart lighting system is divided into 161 lighting zones (N_{lights}), and each zone is considered a controllable load. Dimming the controllable lighting system during the time that the zone is occupied could lead to the user's discomfort, hence a penalty cost $\rho_c = 0.067$ is associated to the lighting load curtailment during the occupied mode. The continuous variable for lighting, $0 \leq \beta^l(k) \leq 0.15$, represents the percentage of dimming associated to each lighting fixture at each sampling time. The maximum percentage of lighting load curtailment is chosen based on Section 130.1(e) of Title 24 [29], which requires that buildings with larger than ten thousand square feet of conditioned space have the capability to respond to a standard DR signal to reduce load up to 15%.

2.3.2 IoT Network of Plug-in Loads

The Plug Load Controller works with sensors in the Enlighted System to transform common power outlets into smart receptacles, see Figure 13. It can be managed from the Enlighted Energy Manager, which turns off power to selected outlets (like task lights, fans, and heaters) at scheduled times, or when a room becomes unoccupied. This reduces passive energy use from idle devices. The Enlighted Plug Load Controller also:

- Collects and aggregates data on plug load electricity usage via the Enlighted Energy Manager for better analysis and decision-making
- Reduces waste heat from idle plug loads (which decreases HVAC costs)
- Helps meet Title 24 obligations by providing an additional reduction source when a demand response (DR) signal arrives from your local utility.
- Leverages Title 24 obligations by integrating DR and BAS (building automation systems) for maximum cost saving

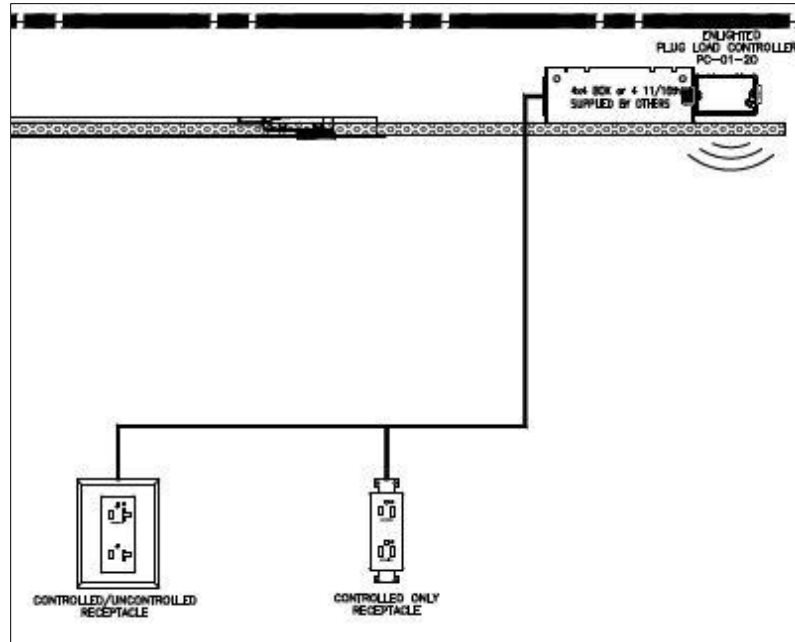


FIGURE 13: Plug load controller layout [26]

The Plug Load Controller enables energy savings by controlling plug loads through occupancy or schedule-based on/off control of receptacles on a circuit. The device is paired with a sensor or a group of sensors in the network to enable occupancy-based control. When an occupant switches on the lights, the plug load controllers energize the power outlets as soon as they receive the ‘Lights ON’ signal from the energy manager indicating that the room is being utilized. When all the occupants leave the room and the lights are switched off, the plug load controllers de-energize the power outlets after a set time thereby switching off the projector and printer automatically. The controller features two sets of wires to separately power controlled and uncontrolled outlets, so that energy consumption on both uncontrolled and controlled circuits are separately measured.

Below are the advanced features of the Plug Load Controller:

- Easily configure and manage plug load behavior by adjusting software profiles for
- individual plug load controllers via the Energy Manager

- Generate reports on outlet outages, carbon reduction, energy and financial savings
- Control capability is up to 20A
- Supports overrides for Demand Response or holiday events
- Utility grade metering chip measures controlled and uncontrolled circuits simultaneously
- Use of industry standard communication protocols provides robust and mature capabilities
- AES 128-bit encryption for wireless data transmission
- SSL encryption for TCP/IP data transmission
- Password protected access control
- Group circuits or functional loads for coordinated control of plug loads
- Configurable with Energy Manager for scheduled or occupancy-based control
- Gain visibility into historical usage patterns with reporting and trending capabilities in the Energy Manager.



FIGURE 14: Enlighted Plug Load Controller installed at ECS 411.

2.3.2.1 Optimal placement of smart plug controllers

As shown in Table 2, there are 820 electrical outlets, without considering the power strip outlets in the ECS building. However, the CEC research grant will only assist CSULB facility management to replace up to 400 smart plug controllers. We need to identify the optimal combination of replacing smart plugs to maximize the overall energy reduction in the ECS building. Resource limitation and lack of energy profile of outlets leads the smart plug controller allocation problem to become a conundrum. In addition, the overall energy reduction is not an identification for demand response capability. To remedy these problems, in the next sub-section we introduce a model-based optimization approach.

2.3.2.2 Model-based optimization protocol for smart plug placement

To determine the optimal location of smart plugs, we first prepare a complete inventory of the building and classify the outlets based on their electric plug loads. There are five types of plug loads in the building: 1) Schedulable plug loads, such as projectors, printers, and LCD screens; 2) Noncritical plug loads, such as computers in laboratories and classrooms; 3) Open plugs, not connected to any fixed load; 4) Critical plug loads, such as severing must-run machines, specialized equipment in the laboratories, and clusters that are always operating; 5) Non-replacing plugs, those that are not considered to be replaced since only one smart plug is being replaced for each faculty room on 5th and 6th floor. Table 4 shows the type and number of plugs in each category.

Based on the plug loads classification, we can develop a weight matrix, which identifies the priority for installing smart plug controllers. For instance, schedulable loads have the highest priority, since they are not frequently used and can be turned on/off during demand response events and/or for energy efficiency measures. Non-critical loads are considered as the second

priority, because they can be turned off when not in used. On the other hand, critical plug loads have the least priority, since they serve must-run loads. Plug loads of these 5 categories belong to 7 different zones which are classified based on the space utilization (classroom, lecture hall, research/technical lab, faculty office, conference room, department office, restroom). Table 5 shows the installation-priority weight for each category.

A model-based optimization approach is developed based on the installation-priority weight matrix [28]. Equations (2.1) to (2.5) summarize the proposed model-based optimization method:

$$\max \sum_{i=1}^{|M|} \sum_{j=1}^{|Z|} \sum_{k=1}^{|N|} W_{ij} X_{ijk} \quad (2.1)$$

$$\text{s. t. } \sum_{i=1}^{|M|} \sum_{j=1}^{|Z|} \sum_{k=1}^{|N|} X_{ijk} \leq 400 \quad (2.2)$$

$$X_{ij} = 0 \text{ or } 1 \forall i \in \{\text{Plug Load Category}\} \quad (2.3)$$

$$W_{1j} \geq W_{2j} \geq \dots \geq W_{Mj} \quad (2.4)$$

$$1 \leq \sum_{i=1}^M \sum_{k=1}^{N_{ij}} X_{ijk} \leq \frac{N_j}{2} \quad j \in \{Z_1\}$$

$$\vdots$$

$$1 \leq \sum_{i=1}^M \sum_{k=1}^{N_{ij}} X_{ijk} \leq \frac{N_j}{2} \quad j \in \{Z_j\} \quad (2.5)$$

where W_{ij} is the installation-priority weight for category M_i belong to zone Z_j , and N_{ij} is the total number of plugs in category M_i belong to zone Z_j . Zones are affecting the installation-priority weight since classrooms, lab rooms and lecture halls have higher priority than other zones, and restroom have the least priority. Equation 5 presents the constraint that zones with

schedulable plug loads should have at least one controllable plug and at most 50% of all plugs in the rooms belong to those zones.

TABLE 5. ECS Buildings Plug Load Inventory

Plug Load Category	Schedulable Plug Loads		Non-Critical Plug Loads		Open Plugs	Non-replacing Plugs (on 5 th /6 th floor)	Critical Plug Loads
	Energy Efficient	Demand Responsive	Energy Efficient	Demand Responsive			
Numbers of Plug Loads	154	17	57	0	228	306	58
Installation-Priority Weight	4	4	3	3	2	1	0

The model-based optimization method allows us to narrow down our search and limit it to three plug load categories: Schedulable plug loads; Non-critical plug loads; and, open plugs. We prioritize open plugs based on their location in the building. For instance, classrooms, lecture halls, and lab rooms have high priority, because these plugs are used frequently for charging students' laptops, phones, and other portable electronic devices. Using our plug loads inventory as the input, half of the schedulable and non-critical plug loads will be replaced by smart plug load controllers because these categories are available in all rooms (except restrooms and exhibition room), which count for 114 smart plugs. Excluding 42 open plugs in the exhibition room, and 12 open plugs in restroom since they are hardly used, the number of open plugs can be replaced is 87. Therefore, the total number of smart plugs should be installed to provide highest opportunity of energy efficiency, demand response capability and cost saving is 201, which is just about 24% of the total number of outlets in the building.

2.4 The IoT-based Building Energy Management System (BEMS)

The ECS building's new Energy Management System will comprise of the existing BMS and the new EMS implemented by Siemen's TNM 8000 which will be supported by Enlighted's BACnet network and sensors. The sensors provided by Enlighted are positioned with the lighting fixtures throughout the building, dividing it into 96 zones that can be individually controlled. These sensors measure various parameters of a room such as the temperature, lighting level and occupancy and transmit the collected data to the Energy Manager via the Gateway. The Gateway further sends the data to the TNM 8000 controller.

The Enlighted Lighting BACnet/IP interface enables BACnet/IP based integration between the Enlighted lighting control network and any BACnet® compatible Building Energy Management System (BEMS). Figure 15 shows that interactions between existing BEMS, new BEMS, and the Enlighted system. With the communication protocol between the two EMS being Niagara, and the new system using BACnet.

The IoT-based BEMS network architecture for the Building's lighting, outlet and HVAC will be composed of 3 main controllers: Tridium TNM8000, Tridium Java Application Control Engine 6 (JACE 6) and Enlighted Network Controller. The Tridium TNM 8000 controller will receive data from Enlighted Network Controller (occupancy data) and from Control Works' Tridium JACE 6 (HVAC sensors and actuators). The TNM8000 controller will then process the data and send commands to the JACE 6 and Variable Frequency Drivers (VFD). The occupancy data is collected from the smart sensors installed at fixtures and is already processed by Enlighted system for controlling smart lighting system. This data transferring process emphasizes how data from Enlighted system be integrated, support, and enhance new smart HVAC system.

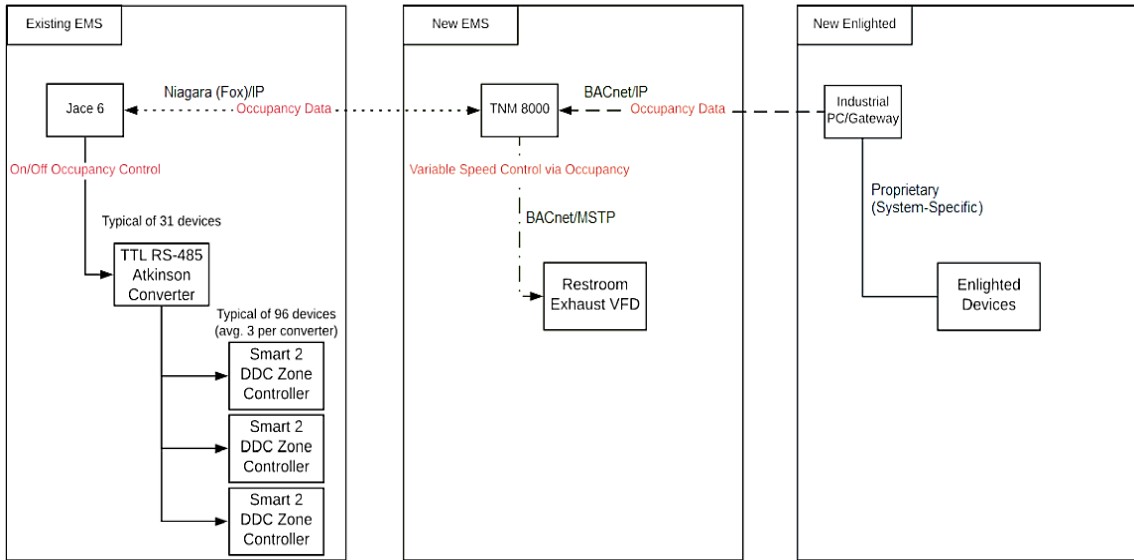


FIGURE 15: Diagram of Interaction of the Existing EMS, New EMS, and The Enlighted System.

The main trunk of the architecture depicted in Figure 15 will be mainly based on BACnet protocol. However, several routers will be used to interface Master Slave Token Passing (MS/TP), Internet Protocol (IP) and Ethernet. The Atkinson Converter will be used to convert Transistor/Transistor Logic into RS485 or EIA 485 from the JACE 6 to Direct Digital Control (DDC) zone controller. The Tridium TNM 8000 runs on Niagara 4 Operating System (OS).

In the current BMS, the system utilizes a static schedule i.e. once any part of the building is occupied, the current BMS will operate the HVAC in all the zones to maintain the desired level of cooling and heating irrespective of the occupancy level, leading to excessive energy consumption and incurring costs. Also, the restroom exhaust currently runs at full speed, any time the building is occupied.

The IoT-based BEMS will still utilize a static schedule, which allows occupancy of the building zones based on time of day. Data from the Enlighted system will be integrated to the existing EMS through the TNM 8000 controller, recognizing un-occupied zones among 96 zones

in the building, via the 31 media converters. In this way, areas can be closed to save HVAC energy in areas that aren't physically occupied. A VFD will be added to the restroom exhaust fan, further reducing energy use by allowing the fan to run at a lower, more efficient speed when the restrooms are unoccupied.

Another major advantage of integrating lighting and HVAC with a single BMS is a faster and better responsive Demand Response strategy. The lighting system can deliver a faster load reduction as compared to the HVAC system which by itself tends to be sluggish with an extensive time lag between changes made to the HVAC setting and the desired result. Attempting to aggressively respond to a load shedding or demand event using only HVAC may result in uncomfortable building environment and may possibly incur peak charges. Thus, in the new BMS, integrated with the Enlighted's BACnet network, sensor devices and existing BEMS allows the HVAC system to achieve any major load adjustment and the lighting network to deliver fine tuning to accomplish optimal demand response.

The IoT-based BEMS system co-optimizes the IoT-based controllable loads with on-site DERs, while considering environmental conditions, occupant comfort, and the utility grid status. Figure 16 presents the principles of the operation of the IoT-based BEMS system. The smart sensors measure occupancy, active motion, ambient light, temperature, and energy consumption of lighting fixtures and plug-in loads. Then, it processes the information locally and creates a rich set of information. This energy, environmental and occupancy information is transferred wirelessly through the Gateway to the Energy Manager for analysis and reporting. The Gateway also communicates configuration changes from the Energy Manager to smart sensors. The Energy Manager provides a secure web-based interface to monitor, manage, and analyze energy savings and other data collected by the smart sensor network, as mentioned previously.

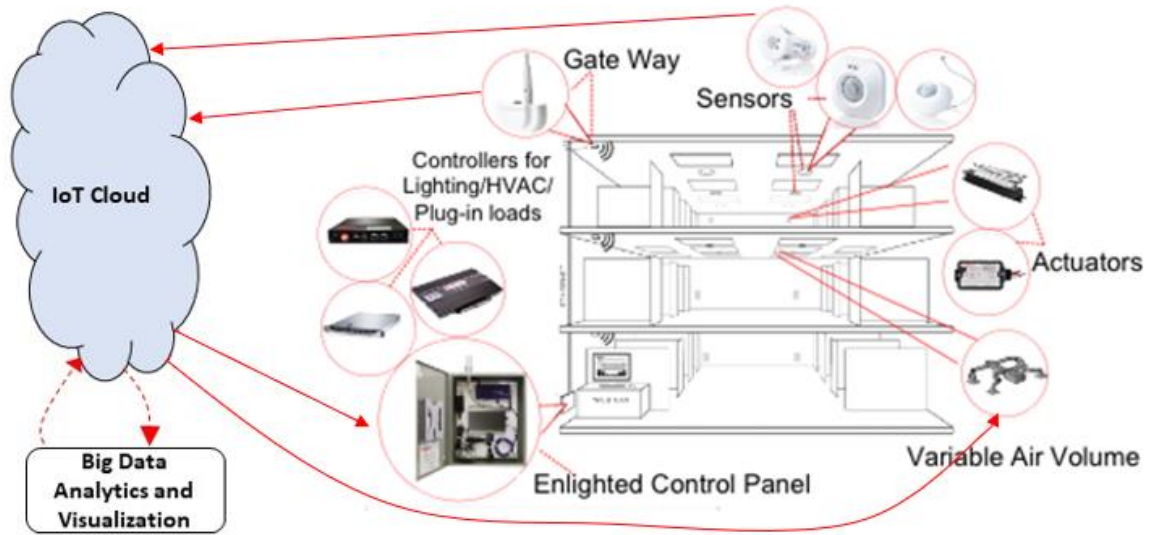


FIGURE 16: Principles of IoT-based BEMS for ECS building

The IoT-based BEMS provides important information about the building utilization, Figure 17. It also provides the hot spot tracking and lighting consumption map of the building. Figure 18 illustrates the average occupancy heat map of the 4th Floor in the ECS building for one academic month, which tells us which zone in that floor has been occupied the most during a specific period.



FIGURE 17: Average space utilization of the ECS building from Jan. 15 to Feb. 15, 2019 [31].



FIGURE 18: Occupancy heat map of the 4th floor in the ECS building from Jan. 15 to Feb. 15, 2019 [32]

CHAPTER 3

BUILDING MICROGRID MODELING AND ANALYSIS

3.1 Distributed Generator Modeling

When a DG unit is operating (or ‘ON’), it would generally have a range of power from which it can output, with a maximum power output P_{max}^{DG} and a minimum power output P_{min}^{DG} . Otherwise, the DG unit is not operating (or ‘OFF’) and would have a power output of zero watts. Therefore, the power output of the DG unit is defined as follows:

$$P^{DG} \in \{ \mathbb{R} | P_{min}^{DG} \leq P^{DG} \leq P_{max}^{DG} \text{ OR } P^{DG} = 0 \} \quad (3.1)$$

The unit commitment variable x^{DG} is assigned to indicate when the DG unit is ‘ON’ ($x^{DG}=1$) or when it is ‘OFF’ ($x^{DG}=0$). Thus, the unit commitment variable is a binary variable; that is, $x^{DG} \in \{0,1\}$. This relationship can be described by the following set of linear inequalities for a time step k , where each of them represents the lower and upper power generating unit:

$$P_{min}^{DG} \cdot x^{DG}(k) \leq P^{DG}(k), \quad \forall k \quad (3.2)$$

$$P^{DG}(k) \leq x^{DG}(k) \cdot P_{max}^{DG}, \quad \forall k \quad (3.3)$$

To directly connect DG power output to fuel cost, let CP be defined as the cost of the fuel consumed by the DG unit at a steady-state power output PDG for a fixed time period. This fuel cost per time period is typically described with the following quadratic form, known as the quadratic cost curve (QCC) [33]:

$$C^P(P^{DG}) = a_1(P^{DG})^2 + a_2(P^{DG}) + a_3, \quad P_{min}^{DG} \leq P^{DG} \leq P_{max}^{DG} \quad (3.4)$$

where a_1 , a_2 , and a_3 are the fuel cost coefficients. This QCC equation is illustrated in Figure 19. A more suitable approach to implement equation (3.4) is provided in [33] and [34]

where the QCC curve is linearized into N piecewise linear segments in equipartition to achieve a linear approximation of the curve, Figure 20.

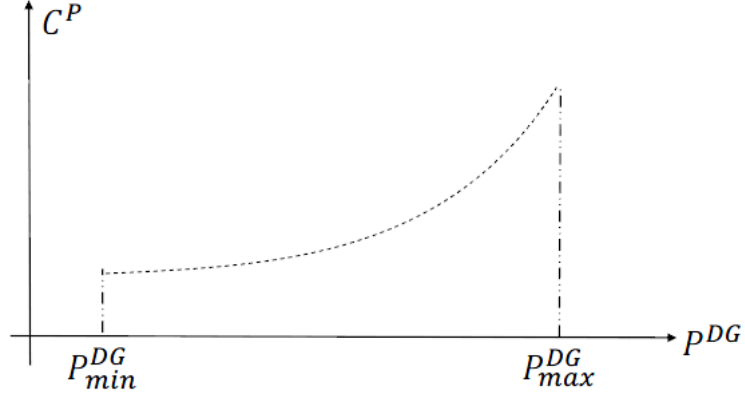


FIGURE 19: The quadratic cost curve (QCC)

The unit's QCC is determined based on the partial load performance in fuel consumption units of BTU/hr [35]. With the price per BTU is \$2.56/million BTU [36], the fuel consumption cost per hour [\$/hr] can be calculated. This data is correlated with the corresponding DG unit power output. Using *polyfit* function in Matlab, the fuel coefficient $a_1[\left(\frac{\$}{kWh}\right)^2]$, $a_2[\left(\frac{\$}{kWh}\right)]$, and $a_3[\frac{\$}{hr}]$ can be determined as:

$$C^P(P^{DG}) = -0.0001(P^{DG})^2 + 0.0294(P^{DG}) + 0.2410 \quad 0 kW \leq P^{DG} \leq 65 kW \quad (3.5)$$

Figure 21 shows the plot of the QCC and the superimposed linearize segments.

The DG startup variable x^{SU} and shutdown variable x^{SD} are now introduced for indicating when the DG unit has been turned off or on; and they are defined as binary since these are indicator variables, so $x^{SU}, x^{SD} \in \{0,1\}$. $x^{SU}(k)$ is set to 1 at time step k if the DG unit was turned on at time step k when it was previously off at time step k-1, and $x^{SU}(k)$ is set to 0 otherwise. The shutdown variable x^{SD} is defined similarly.

$$x^{DG}(k) - x^{DG}(k-1) \leq x^{SU}(k) \leq 1, \quad \forall k \quad (3.6)$$

$$x^{DG}(k-1) - x^{DG}(k) \leq x^{SD}(k) \leq 1, \quad \forall k \quad (3.7)$$

The costs associated with starting up and shutting down the DG are defined as:

$$SU(k) = c^{SU}(k)x^{SU}(k), \quad \forall k \quad (3.8)$$

$$SD(k) = c^{SD}(k)x^{SD}(k), \quad \forall k \quad (3.9)$$

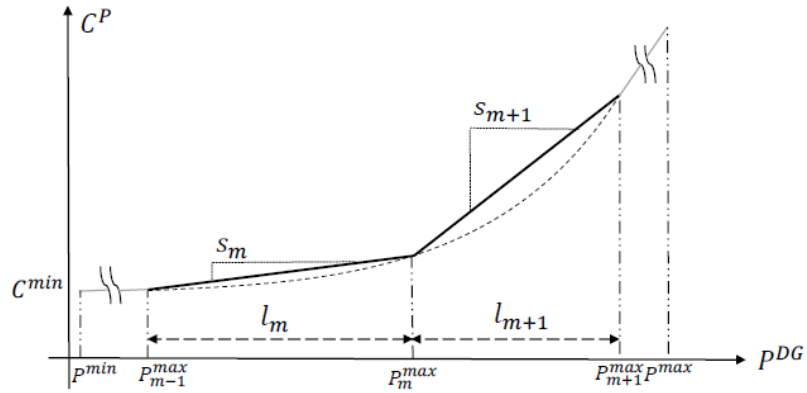
$$SD(k), SU(k) \geq 0, \quad \forall k \quad (3.10)$$


FIGURE 20: Piecewise linear approximation for the quadratic cost curve.

There is also an operation and maintenance cost due to technical services and part replacement, and is defined by the following equation:

$$OM(P^{DG}(k)) = c^{OM} P^{DG}(k) \quad (3.11)$$

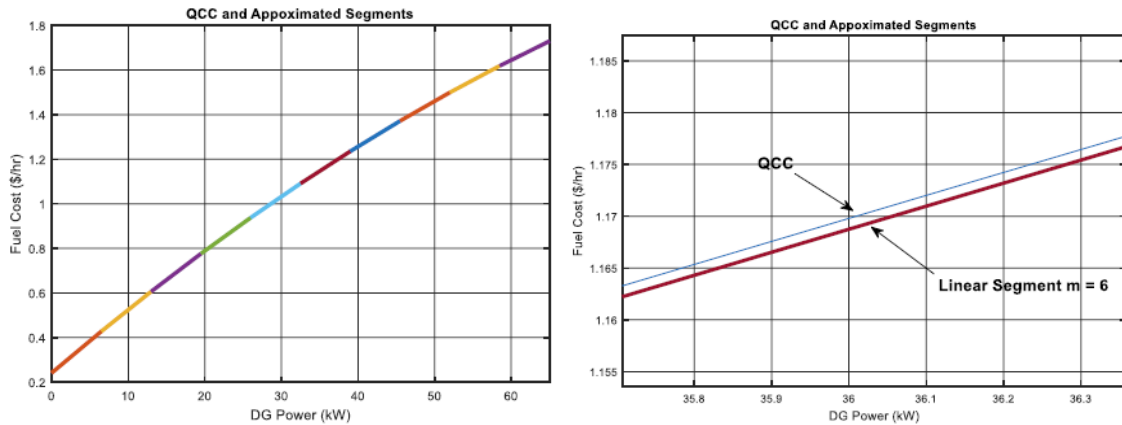


FIGURE 21: The QCC and the superimposed linearize segments.

A detail discussion regarding the DG unit commitment, the nonlinear relationship between the fuel consumption cost, minimum uptime/downtime, power ramping can be find in [37].

A Capstone C65 Micro-Turbine (MT), Figure 22, is chosen for the proposed ECS building microgrid. This natural gas MT provides 2 minutes start-up and 10 minutes cool-down process, and it has power ramping limit at 65 kW/15-minutes, or 260 kW/hr. This MT also has a very low maintenance cost which is about \$0.003 per kWh. This MT also has following advancements:

- Ultra-low emissions
- One moving part – minimal maintenance and downtime
- Patented air bearings – no lubricating oil or coolant
- Integrated utility synchronization – no external switchgear
- Compact modular easily combined – act as single generating source
- Remote monitoring and diagnostic capabilities
- Proven technology with tens of millions of operating hours

The general specifications of the chosen MT are:

- Rating: 65 kW
- Electrical Efficiency LHV: 29%
- Voltage: 400-480 VAC
- Frequency: 50/60 Hz
- Electrical Service: 3-phase, 4-wire Wye
- Dimension: width (30 inch), depth (77 inch), height (75 inch)
- Weight: grid connect – 1,671 lb

- Net heat rate LHV: 12.4 MJ/kWh (11,800 BTU/kWh)
- Exhaust Temperature: 309°C (588°F)
- Exhaust gas flow: 0.49 kg/s (1.08 lbm/s)
- Compatible fuels: natural gas, liquid fuel, biogas, propane gas



FIGURE 22: Capstone Micro-Turbine C65

More detail of this MT such as engine components, engine and exhaust characteristics can be found at [38].

3.2 Energy Storage Modeling

Let $x^b(k)$ be denoted as the energy in the storage device at time step k in units of kWh, and is bounded to the upper x_{max}^b and lower x_{min}^b limit capacity of the storage. $P^b(k)$ is denoted as the storage power exchange at time step k , η is the power exchange efficiency, and x^{sb} is the storage energy degradation. The energy storage model is described as follows:

$$x^b(k + 1) = x^b(k) + \eta P^b(k) \Delta t - x^{sb} \Delta t \quad (3.12)$$

with

$$x^b \in \{\mathbb{R} | x_{min}^b \leq x^b \leq x_{max}^b\} \quad (3.13)$$

A binary decision variable $\delta^b(k)$ is utilized to determine if the storage device is charging ($P^b(k) \geq 0$) or discharging ($P^b(k) \leq 0$) at time step k . The relationship between δ^b and P^b can be described as an if and only if statement: $P^b(k) \geq 0 \Leftrightarrow \delta^b = 1$. The storage charging efficiency η^{ch} and discharging efficiency η^{dis} are within the boundary of 0 to 1. The new description of equation can be described as follows:

$$x^b(k+1) = \begin{cases} x^b(k) + \eta^{ch}(P^b(k)\Delta t - x^{sb}\Delta t), & \delta^b = 1 \text{ (charging mode)} \\ x^b(k) + \frac{1}{\eta^{dis}}(P^b(k)\Delta t - x^{sb}\Delta t), & \delta^b = 0 \text{ (discharging mode)} \end{cases} \quad (3.14)$$

This nonlinear conditional statement is needed to be transferred to a linear equation in order to describe in a MILP optimization problem. A supplementary decision variable $z^b(k) = \delta^b(k)P^b(k)$ is utilized to do this work. Following [22] and [39], the energy storage can be described linearly with following equation:

$$x^b(k+1) = x^b(k) + \left(\eta^{ch} - \frac{1}{\eta^{dis}}\right)z^b(k)\Delta t + \frac{1}{\eta^{dis}}P^b(k)\Delta t - x^{sb}\Delta t \quad (3.15)$$

Note that $z^b(k)$ hides the nonlinearity $\delta^b(k)P^b(k)$ in this equation.

The “if..then” statement, or logical statement, can be described linearly using a mathematical technique [37], since it would be appropriate for implementation onto the MILP inequality constraints. The following gives an equivalent for the logical statement and inequality constraint; with δ as a binary indicator, tolerance ε , function f , real value m and M such that $f \in \{\mathbb{R} | m \leq f \leq M\}$, equation x and x are equivalent:

$$f(k) \geq 0 \Leftrightarrow \delta^b = 1 \quad (3.16)$$

and

$$\begin{cases} -m\delta \leq f(k) - m \\ -(M + \varepsilon)\delta \leq -f(k) - \varepsilon \end{cases} \quad (3.17)$$

Moreover, with real function y , equation x and x are equivalent:

$$y = \delta f(k) \quad (3.18)$$

and

$$\begin{cases} y \leq M\delta \\ y \geq m\delta \\ y \leq f(k) - m(1 - \delta) \\ y \geq f(k) - M(1 - \delta) \end{cases} \quad (3.19)$$

Therefore, the following set of linear inequality constraints are utilized to describe both the if and only if dynamic between P^b , z^b , and δ^b and the product relationship of the three terms:

$$\begin{cases} C^b \delta^b(k) \leq P^b(k) + C^b, \forall k \\ -(C^b + \varepsilon) \delta^b(k) \leq -P^b(k) - \varepsilon, \forall k \\ C^b \delta^b(k) + z^b(k) \leq P^b(k) + C^b, \forall k \\ C^b \delta^b(k) - z^b(k) \leq -P^b(k) + C^b, \forall k \\ -C^b \delta^b(k) + z^b(k) \leq 0, \forall k \\ -C^b \delta^b(k) - z^b(k) \leq 0, \forall k \end{cases} \quad (3.20)$$

With ε as the machine precision, and C^b as the maximum power flow to or from the energy storage unit.

A set of three Aspen 48M-25.9 batteries [40] are placed in parallel to create the energy storage system for the proposed ECS building microgrid. We have analyzed that placing three batteries in parallel would provide the most benefit, since adding more batteries will result in underutilization and minimal increase in operational cost savings, Figure 24. The batteries have almost no operation and maintenance costs during their 3000-cycle lifespan (to 70% retained capacity).



FIGURE 23: Aspen 48M-25.9 saltwater battery bank

The advancements of this battery bank include:

- Reliable:
 - Avoid costly downtime and battery replacement
 - Tolerant to high ambient temperatures
 - 100% DoD cycling with minimal degradation
 - Self-balancing, minimal self-discharge, and no trickle charge required
 - High tolerance to long stands at partial state of charge
- Safe and non-toxic
 - Safe to handle, ship, and operate
 - Non-flammable, non-toxic, and non-explosive
 - No dangerous or catastrophic failure modes
 - Eliminates high concentrations of toxic or flammable materials
- Cost effective
 - Excellent calendar and cycle life
 - No thermal management or active battery management system required

- Simple system operation
- Minimal system maintenance
- Sustainable
 - Environment friendly
 - No hazardous or toxic materials
 - Recyclable and land-fill safe

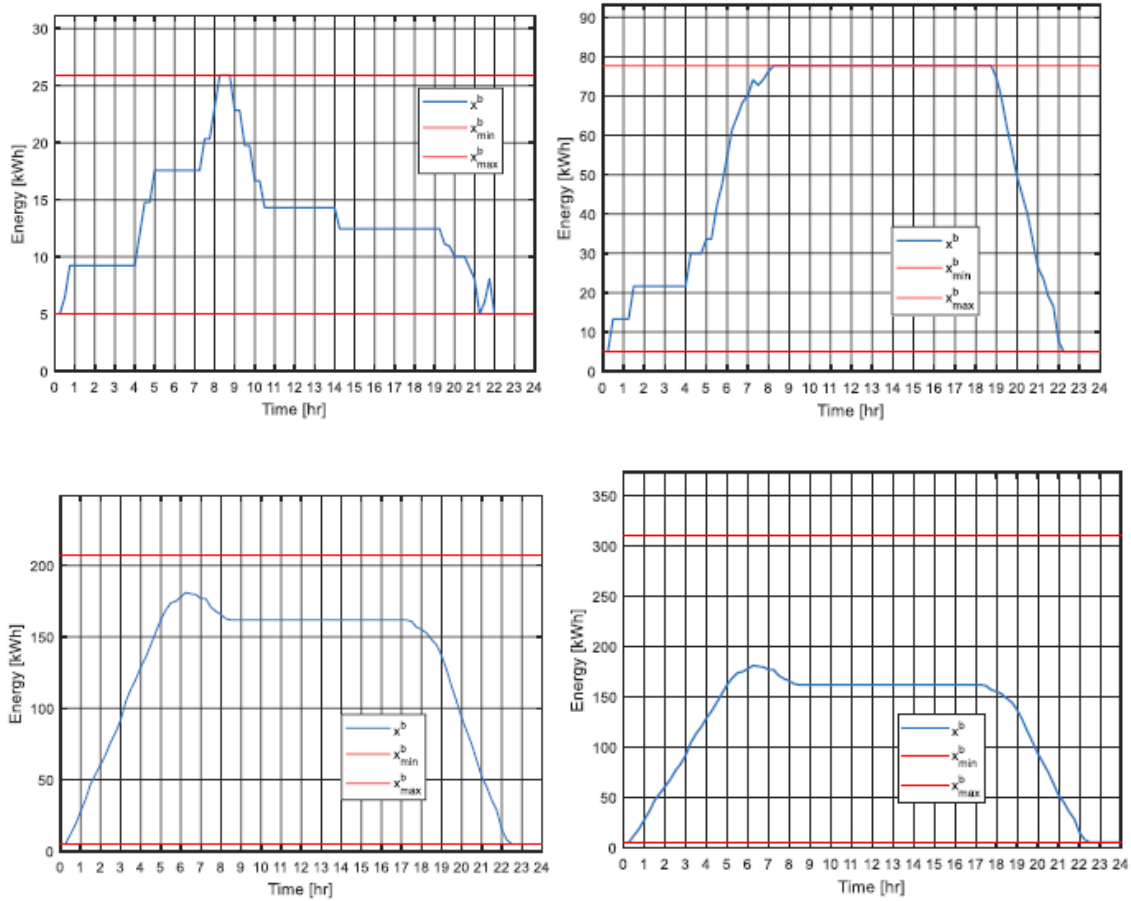


FIGURE 24: x^b plot with: 1 battery, 3 batteries, 12 batteries.

The general specifications of this battery bank are:

- Nominal battery voltage: 48 V
- Nominal capacity: 25.9 kWhr

- Cycle life: 3000 cycles (up to 70% retained capacity)
- Voltage range: 40 – 59.5 V
- Peak power: 11.7 kW
- Dimension: height (45.6 inch), width (52 inch), depth (40 inch)
- Weight: 3,315 lbs

Based on the storage energy degeneration is obtain in Figure 25 [40] with the monthly capacity loss as a function of the ambient temperature, a self-discharge of 10% of the storage capacity occurs each month if placing the batteries in room temperature (20⁰C). Since we have three Aspen 48M-25.9 placed in parallel which creating a combined capacity of 77.7 kWh, we will have a self-discharge of 7.77 kWh/month. This translates to 0.0027 kWh/15-min for a 31 days month.

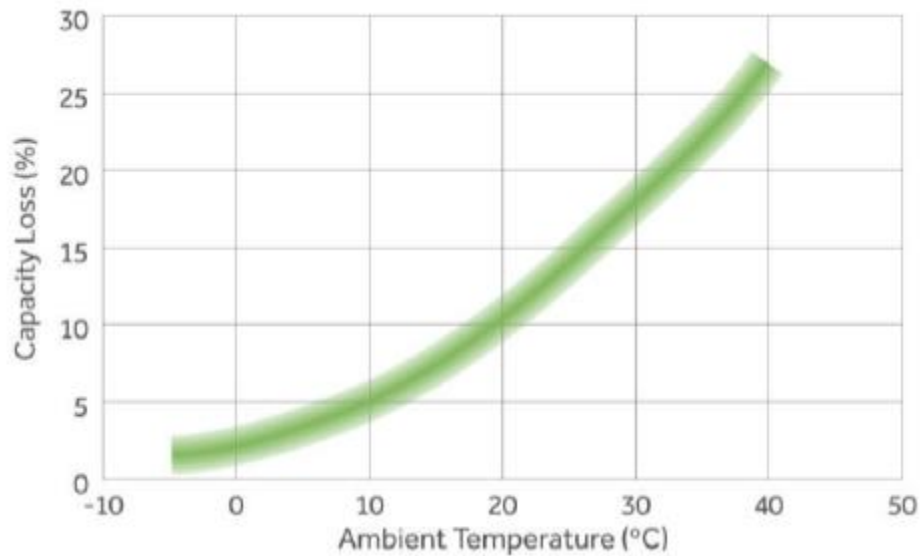


FIGURE 25: Self-discharge of Aspen 48M-25.9 battery over a month.

For x^b , to avoid having battery discharge at 0%, the lower bound and end target are chosen to be 5 kWh. Since the round-trip efficiency is 90%, the in-and-out efficiency is:

$$\eta^{ch}\eta^{dis}P = \eta^2P = \eta^{roundtrip}P = 0.9P$$

Therefore,

$$\eta = \sqrt{0.9} = 0.95 = \eta^{ch} = \eta^{dis}$$

3.3 Utility Grid Modeling

The proposed building microgrid can purchase electricity from the utility grid and sell back electricity to the grid. To model the utility grid power purchase, a binary state variable $\delta^g(k)$ is introduced that determines if the user is purchasing energy ($P^g(k) \geq 0$) or selling energy ($P^g(k) \leq 0$) to the grid. Therefore, the relationship between δ^g and P^g can be described as an if and only if statement: $P^g(k) \geq 0 \Leftrightarrow \delta^g = 1$. The price of electricity at time step k is $C^P(k)$, and the selling price is $C^S(k)$, both converted to \$/kW. The resulting model is a logical conditional statement as follows:

$$C^g(k) = \begin{cases} C^P(k)P^g(k), & \delta^g(k) = 1 \\ C^S(k)P^g(k), & \delta^g(k) = 0 \end{cases} \quad (3.21)$$

Similar to energy storage dynamics, the linearized equivalent of equation x is as follow:

$$T^g \delta^g(k) + z^g(k) \leq P^g(k) + T^g, \quad \forall k \quad (3.22)$$

$$-(T^g + \varepsilon) \delta^g(k) \leq -P^g(k) - \varepsilon, \quad \forall k \quad (3.23)$$

$$M^g \delta^g(k) + C^g(k) \leq C^P(k)P^g(k) + M^g, \quad \forall k \quad (3.24)$$

$$M^g \delta^g(k) - C^g(k) \leq -C^P(k)P^g(k) + M^g, \quad \forall k \quad (3.25)$$

$$-M^g \delta^g(k) + C^g(k) \leq C^S(k)P^g(k), \quad \forall k \quad (3.26)$$

$$-M^g \delta^g(k) - C^g(k) \leq -C^S(k)P^g(k), \quad \forall k \quad (3.27)$$

with T^g is the maximum power flow to and from the utility grid and $M^g = \max \{C^P(k), C^S(k)\} \cdot T^g$.

The forecast profiles of $C^P(k)$ and $C^S(k)$ can be obtained from the TOU rates supplied by the energy service provider, which is SCE in this case.

3.3.1 Peak demand cost modeling

A peak demand cost model is needed to be implemented to the MILP optimization because utility companies bill their large customers for peak demand use to offset the cost of supplying high amount of power and encourage customers to reduce consumption during peak hours. The peak demand cost can be described as follows:

$$J^{peak} := \max \{P^g\} \cdot c^{peak} \quad (3.28)$$

Where P^g is the set of all power grid instances chosen by the optimization approach and c^{peak} is the cost coefficient in \$/kW. To linearize the maximum function, a supplementary variable Z^g , which represents the maximum power instance of P^g , is used. The variable Z^g replaces the nonlinear term $\max \{P^g\}$ in the objective function. The linear peak demand cost model can be described by the following set of linear inequalities:

$$J^{peak} := Z^g \cdot c^{peak} \quad (3.29)$$

$$P^g(k) \leq Z^g, \quad \forall k = 1, \dots, T \quad (3.30)$$

3.3.2 Energy balancing modeling

To ensure that all power supplying components of the building satisfy the user's power demands, the following energy balancing equivalence is established:

$$P^{DG}(k) + P^{PV}(k) + P^g(k) - P^b(k) = D(k) + \sum_{h=1}^{N_{lights}} [1 - \beta_h^l] D^l(k), \quad \forall k = 1, \dots, T \quad (3.31)$$

Note that P^{DG} , P^b , and P^g are decision variables while P^{PV} , D , and D^l are determined through forecasting. Since the forecast solar power and forecast demand profiles are implemented to the optimization problem, it would be more precise to use the predicted PV output \hat{P}^{PV} and demand \hat{D} , and \hat{D}^l to the energy balancing model.

$$P^{DG}(k) + \hat{P}^{PV}(k) + P^g(k) - P^b(k) = \hat{D}(k) + \sum_{h=1}^{N_{lights}} [1 - \beta_h^l] \hat{D}^l(k), \quad \forall k = 1, \dots, T \quad (3.32)$$

This discrete equation describes a real-world continuous-time dynamic, and continuous-time data like PV power must be discretized before implemented to the equation.

3.4 PV Power Profile and TOU Rate

3.4.1 PV profile

The PV power profile is given as a continuous-time model and it need to be converted to discrete-time model profile in order to apply to MILP optimization. This process can be done using a Zero-Order Hold (ZOH) approach on the PV power profile. With T_s is the sampling period for the PV profile, the following sample-and-hold equation is utilized:

$$P^{PV}(t) = P^{PV}(k), kT_s \leq t \leq (k + 1)T_s, \forall k = 1, \dots, T \quad (3.33)$$

where $P^{PV}(k)$ is the historical data of the PV power profile. The implementation of the ZOH approach on the continuous-time profile is illustrated in Figure 26.

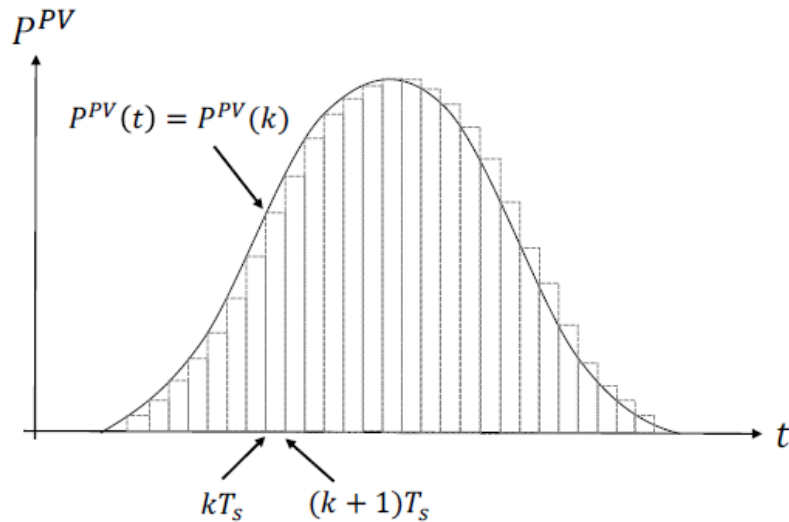


FIGURE 26: PV power profile discretized using ZOH.

Since the desired sampling period for MILP optimization problem is 15-minutes, the PV power profile after being discretized should also have 15-minutes sampling period.

The active power profile of May 11st, 2017 is used because it has clear weather on that day thus provided an ideal PV power profile. The roof area of ECS building is 14,362 sqft, therefore a 105 kWh PV system is designed for the proposed ECS building microgrid.



FIGURE 27: Proposed PV system on the roof of the ECS building.

3.4.2 TOU rate

Typically, the utilities company will inform their customers of the energy price rates and both parties will agree upon them through bilateral contracts before services. These rates vary by season, day of week, and time of day. There are usually two rates, known as On-Peak hours rate (during evening period when there is high customer demand), and Off-Peak hours rate (out-side of On-Peak hours). This schedule is known as TOU rate, and it may change depending on the season.

There is no uncertainty in the energy purchasing/selling rate forecast since both parties have agreed on the rates through the contract. The purchasing rate $C^P(k)$ and selling rate $C^S(k)$ can be determined through the TOU schedule.

Retail tariff, to which the CSULB campus is subject to, is SCE TOU-8-B with the average price of electricity of \$0.067/kWh [41], [42]. The purchasing and selling rate are shown in Figure 28, and the rates are given in \$/kW15-min to coincide with the sampling rate.

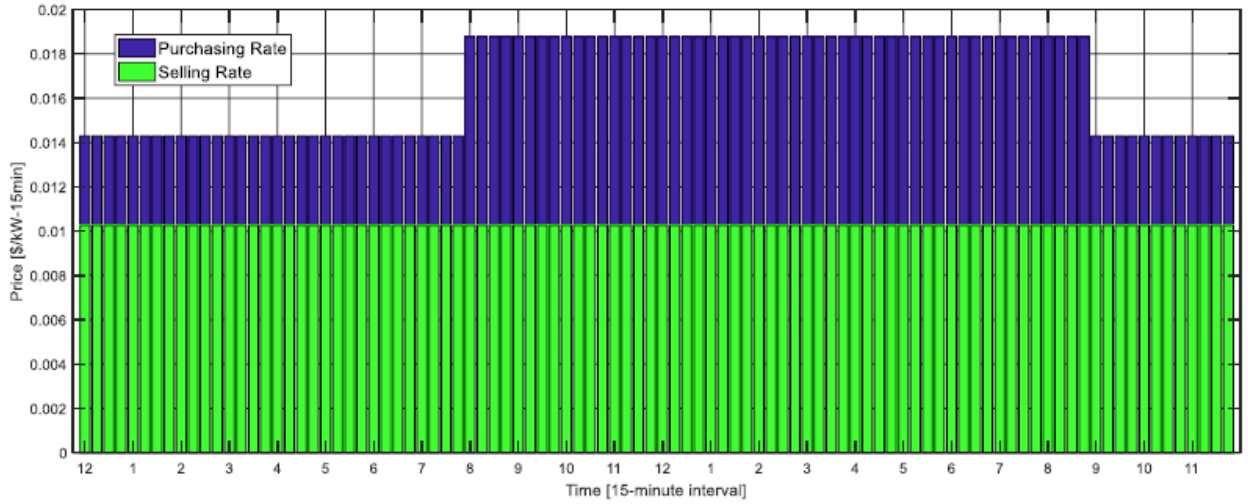


FIGURE 28: SCE TOU-8-B purchasing and selling rate.

3.5 Forecast Uncertainty Modeling

To demonstrate the advantage of the MPC-MILP controller, we must include uncertainties in the PV power and demand forecast. This paper adopts the uncertainty modeling with correlation approach from [43] and extend this work with our formulation to update forecasts at each time step. A zero-mean, normally distributed signal is passed through a causal filter with a finite impulse response to create a deviation. Then this deviation is additively implemented to provided historical data, resulting in our generalized forecast data with uncertainty. The forecast modeling is shown in Figure 29.

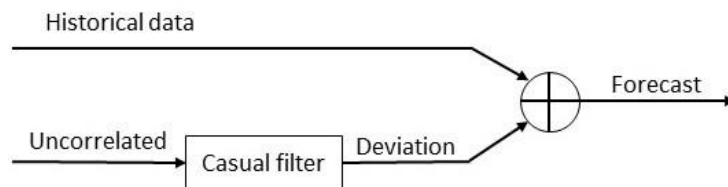


FIGURE 29: Forecast modeling method.

This process begins by defining the historical data sequence $\bar{b} = \{\bar{b}(\tau)\}_{\tau=1}^T$. Uncertainty to \bar{b} is implemented by using a causal filter with finite impulse response $f = \{f(\tau)\}_{\tau=1}^T$. Thus, with $\Delta > 0$, f is defined as follows:

$$f(t) = \begin{cases} 1, & 0 \leq t \leq \Delta \\ 0, & \text{otherwise;} \end{cases} \quad (3.34)$$

A zero-mean, normally distributed signal $e = \{e(\tau)\}_{\tau=1}^T$ is passed through the casual filter resulting in deviation δb :

$$\delta b(\tau) = \sum_{s=1}^T e(s)f(\tau - s), \quad \tau = 1, \dots, T \quad (3.35)$$

Finally, this deviation is additively implemented to \bar{b} , resulting in the generalized forecast with uncertainty $\hat{b}(\tau)$:

$$\hat{b}(\tau) = \bar{b}(\tau) + \sum_{s=1}^T e(s)f(\tau - s), \quad \tau = 1, \dots, T \quad (3.36)$$

Along with forecasting PV power and critical demand, we will also include our formulation to update forecasts at each time step of the controllable loads, with equations (3.37)-(3.39). We want the forecasts to improve in accuracy when it is calculated closer to the predicted event. Therefore, for the critical demand, PV demand, and controllable lighting demand, we define the calculated forecast for time τ predicted at time k as $\widehat{D}(\tau|k)$, $\widehat{P}^{PV}(\tau|k)$, and $\widehat{D}^l(\tau|k)$, respectively. To implement adjustment to these forecasts, we apply a correction convergence filter $h(\tau|k)$ to the forecast with uncertainty as follows:

$$\widehat{D}(\tau | k) = D(\tau) - h(\tau, k) \cdot \delta D(\tau) \quad (3.37)$$

$$\widehat{P}^{PV}(\tau | k) = P^{PV}(\tau) - h(\tau, k) \cdot \delta P^{PV}(\tau) \quad (3.38)$$

$$\widehat{D}^l(\tau | k) = D^l(\tau) - h(\tau, k) \cdot \delta D^l(\tau) \quad (3.39)$$

where, for a finite correction time horizon $H_c > 0$,

$$h(\tau, k) = \begin{cases} 1 - \frac{(\tau - k)}{H_c}, & \tau = k, \dots, k + H_c \\ 0, & \tau > k + H_c \end{cases} \quad (3.40)$$

Note that if the forecast at time step τ is within H_c when the prediction is made, $h(\tau, k)$ causes the error in the demand forecast $\delta D(\tau)$ to converge to 0 at each time step.

CHAPTER 4

CONTROL STRATEGY DEVELOPMENT

The proposed microgrid optimal scheduling should optimally schedule power production from PV solar panels, micro-turbine, storage, as well as controllable loads, in order to supply the microgrid demand and minimize the microgrid's operational cost and the cost of buying electricity from utility grid. This chapter introduces the needed mathematical background to construct the proposed MPC-MILP control approach.

At every time step (each 15 minutes), the MPC-MILP should have solution for the following questions:

- Unit commitment: when should micro-turbine start and stop; when should storage device be charged or discharged.
- Economic dispatch: how much power should each generator generate to cover loads at lowest cost.
- When and how much energy to be purchased from or sold to the grid.
- Which controllable loads should be curtailed and when.

For the simplicity, only two types of loads in the building microgrid are considered for the MPC-MILP control approach:

- Critical loads: loads that must be on for essential processes whenever the occupants want them to be on.
- Controllable loads: load that can be curtailed during demand response or emergency situations (the smart lighting system).

4.1 MILP Principles

Assuming there is a linear function $f(x)$ that is needed to be minimized subject to the argument x . The problem can have constraints that bound x between values in an inequality and equate x as an equality. Suppose a decision vector \mathbf{x} is chosen to represent the set of decision variables that contain both continuous and integer variables:

$$\mathbf{x} := [x_1, x_2, \dots, x_k, \dots, x_n]', x_k \in \mathbb{R} \times \{0,1\}, \forall k \quad (4.1)$$

And the coefficient vector \mathbf{f} is comprised of continuous values:

$$\mathbf{f} := [f_1, f_2, \dots, f_k, \dots, f_n]', f_k \in \mathbb{R}, \forall k \quad (4.2)$$

The objective function of the MILP problem can then be described as:

$$\mathbf{f}^T \mathbf{x} = f_1 x_1 + f_2 x_2 + \dots + f_n x_n \quad (4.3)$$

The variables in the decision vector will have constraints attached to them in the MILP problem, both equalities and inequalities. For instance, with real coefficients $a = \{a_{ik} \in \mathbb{R}, \forall i = 1, \dots, m, k = 1, \dots, n\}$ and $b = \{b_k \in \mathbb{R}, \forall k = 1, \dots, m\}$, a set of linear inequality constraints can be described as follows:

$$\begin{aligned} a_{11}x_1 + a_{12}x_2 + \dots + a_{1n}x_n &\leq b_1 \\ a_{21}x_1 + a_{22}x_2 + \dots + a_{2n}x_n &\leq b_2 \\ &\vdots \\ a_{m1}x_1 + a_{m2}x_2 + \dots + a_{mn}x_n &\leq b_m \end{aligned} \quad (4.4)$$

Compacting the set into matrix-vector form, with $m \times n$ matrix $A = [A_{ik} = a_{ik}]$ and $m \times 1$ vector $B = [b_1, b_2, \dots, b_m]'$, the inequality constraint $A \cdot \mathbf{x} \leq B$ is obtained.

Similarly, the equality constraint and bounding constraint in matrix vector form are as follows:

$$A_{eq} \cdot \mathbf{x} = B_{eq} \quad (4.5)$$

$$lb \leq \mathbf{x} \leq ub \quad (4.6)$$

Where lb and ub is the lower and upper bound vector. The MILP optimization problem can be described as follows:

$$\min_{\mathbf{x}} \mathbf{f}^T \mathbf{x} \text{ subject to } \begin{cases} \mathbf{x}_{int} \subseteq \mathbf{x}, \mathbf{x}_{int} \in \mathbb{I} \\ A \cdot \mathbf{x} \leq B \\ Aeq \cdot \mathbf{x} = Beq \\ lb \leq \mathbf{x} \leq ub \end{cases} \quad (4.7)$$

4.2 Connecting MILP Optimization to Optimal Scheduling

This MILP optimization problem can be translated to an optimal scheduling whose the ultimated goal is to minimize the daily operational cost of the microgrid while satisfying the user's power demand and the microgrid's operation constraints. The optimal scheduling problem can be expressed in words as:

$$\min_{\text{control inputs}} (\text{Costs}) \text{ subject to } \{\text{Microgrid operational constraints}\}$$

The MILP optimization gives a finite number of control decision solution in \mathbf{x} , so the outputs need to be realized as a digital controller with discrete control outputs, where one instance of the command input is implemented to the microgrid's local controllers for a certain time period, then in the next instance a new command is set. Therefore, the decision vector of the MILP problem as a set of all the command inputs to the microgrid local controllers, as well as auxiliary variables from time step $k=1$ to $k=T$, where T is the last time step of the MILP problem's optimization window.

The decision vector for the microgrid optimal scheduling problem can be defined as follows:

$$\begin{aligned} \mathbf{x}(k) = & \\ [P^{DG}(k) \ l_m(k) \ x^{DG}(k) \ x^{SU}(k) \ x^{SD}(k) \ x^b(k) \ P^b(k) \ \delta^b(k) \ Z^b(k) \ P^G(k) \ Z^g \ \beta^{lights}]' \in & \\ \mathbb{R} \times \{0,1\}, \forall k = 1, \dots, T & \end{aligned} \quad (4.8)$$

Where $P^{DG}(k)$ $l_m(k)$ $x^{DG}(k)$ $x^{SU}(k)$ $x^{SD}(k)$ represent the control solutions for DG unit, $x^b(k)$ $P^b(k)$ $\delta^b(k)$ $Z^b(k)$ represent the control solutions for energy storage, $P^G(k)$ Z^g represent the control solution for utility grid, and β^{lights} represents the control solutions for the curtailment level of lighting controllable zones.

Each of the elements of the control solution variables is a vector, and the decision vector can be understood as a vector of vectors. For example, $x^b(k)$ and $P^b(k)$ are defined as follows:

$$x^b = \begin{bmatrix} x^b(1) \\ x^b(2) \\ \vdots \\ x^b(T) \end{bmatrix}, P^b = \begin{bmatrix} P^b(1) \\ P^b(2) \\ \vdots \\ P^b(T) \end{bmatrix}$$

$$x = \begin{bmatrix} \vdots \\ x^b(1) \\ x^b(2) \\ \vdots \\ x^b(T) \\ P^b(1) \\ P^b(2) \\ \vdots \\ P^b(T) \\ \vdots \end{bmatrix} \quad (4.9)$$

Based on the mathematical modeling of microgrid's components, the lower bounds and upper bounds of the decision variables in x can be summarized as follows:

$$P^{DG} \in \{\mathbb{R} | P_{min}^{DG} \leq P^{DG} \leq P_{max}^{DG} \text{ OR } P^{DG} = 0\} \quad (4.10)$$

$$0 \leq l_m \leq (P_m^{max} - P_{m-1}^{max}) \cdot x^{DG}, \forall m \quad (4.11)$$

$$x^{DG}, x^{SU}, x^{SD} \in \{\mathbb{Z} | 0 \leq x^{DG}, x^{SU}, x^{SD} \leq 1\} \quad (4.12)$$

$$x^b \in \{\mathbb{R} | x_{min}^b \leq x^b \leq x_{max}^b\} \quad (4.13)$$

$$P^b \in \{\mathbb{R} | -|P_{ch-max}^b| \leq P^b \leq |P_{diss-max}^b|\} \quad (4.14)$$

$$\delta^b \in \{\mathbb{R} | 0 \leq \delta^b \leq 1\} \quad (4.15)$$

$$z^b(k) \in \{\mathbb{R} | 0 \leq z^b \leq |P_{diss-max}^b|\} \quad (4.16)$$

$$P^g \in \{\mathbb{R} \mid -|T^g| \leq P^g \leq |T^g|\} \quad (4.17)$$

$$\delta^g \in \{\mathbb{Z} \mid 0 \leq \delta^g \leq 1\} \quad (4.18)$$

$$Z^g \in \{\mathbb{R} \mid 0 \leq \delta^b \leq \infty\} \quad (4.19)$$

$$\beta^l \in \{\mathbb{R} \mid 0 \leq \beta^l \leq 0.15\} \quad (4.20)$$

4.2.1 Cost objective function

The cost objective function is used to determine the daily operating cost of the microgrid, which includes DG fuel costs, peak load, maintenance, purchased grid energy, and costs associated with start-up and shut-down of the DG unit. The cost function J is defined as follows:

$$J := \sum_{k=1}^T \left\{ C^{OM} P^{DG}(k) + \sum_{m=1}^N s_m l_m(k) + C^{min} x^{DG}(k) + C^{SU} x^{SU}(k) + C^{SD} x^{SD}(k) + C^g(k) + \rho_c \sum_{h=1}^{N_{lights}=161} \beta_h^{lights}(k) D_h^c(k) \right\} + C^{peak} Z^g \quad (4.21)$$

Where k is the time step instance, N is the number of quadratic cost curve (QCC) segment partition, and T is the time horizon, which is 24 hours at 15-minutes sampling intervals, thus $T=96$.

4.2.2 MILP control system

The optimal scheduling as a MILP optimization problem can now be formalized as follows:

$$\min_x \sum_{k=1}^T \left\{ C^{OM} P^{DG}(k) + \sum_{m=1}^N s_m l_m(k) + C^{min} x^{DG}(k) + C^{SU} x^{SU}(k) + C^{SD} x^{SD}(k) + C^g(k) + \rho_c \sum_{h=1}^{N_{lights}=161} \beta_h^{lights}(k) D_h^c(k) \right\} + C^{peak} Z^g \quad (4.22)$$

subject to:

Fuel cost constraints

DG operation model constraints

- Energy storage model constraints
- Storage Dynamics constraints
- Utility grid interaction constraints
- Energy balancing model constraints
- Bounding constraints

At each time step k , the MILP control system will implement the following command inputs for the microgrid's local controllers:

$$\left\langle \begin{array}{l} P^{DG}(k), x^{DG}(k), P^b(k) \\ \delta^b(k), P^g(k) \end{array} \right\rangle$$

Figure 30 shows the diagram of the open loop MILP control system.

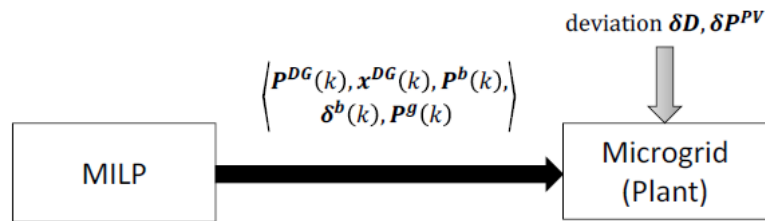


FIGURE 30: MILP control system.

As shown in the Figure 30, even though MILP control system give new command inputs at each time step, they are all calculated with one calculation at the beginning of the day at the latest since there is no form of feedback compensation in this system. Its performance therefore relies heavily on the uncertainty in the critical demand, controllable demand, and PV forecast, which are not always accurate. Therefore, in order to compensate the forecast uncertainties, the implementation of MPC approach in conjunction with MILP is proposed.

4.3 The Proposed MPC-MILP control approach

4.3.1 MPC principles

MPC is an optimal control approach that control dynamic systems subject to its modeling constraints by measuring states from a system plant, calculating a control sequence for a finite horizon, and implementing the first step in the control sequence. The prediction horizon is shift forward at each time step, and the process of the control system is repeated. This online method is proved to have better performance in compare with other offline approach with modeling uncertainties.

MPC optimization has three main properties:

- Dynamic models: $x(k+1)=f(x(k),u(k))$
- Constraints: $x(k) \in X, u(k) \in U$
- Cost: $J(k) = \min \sum_{k+1}^N g(x(k), u(k))$

where $x(k)$ is the state variable with a prediction horizon of W , $u(k)$ is the control sequence with a control horizon of R .

4.3.2 MPC-MILP control strategy

This sub-section introduces in detail the proposed MPC-MILP control approach.

The following inputs need to be given to the MPC-MILP controller before the optimization process begin, including: utility rates $C^P(k), C^S(k), k = 1, \dots, T$, storage energy state $x^b(k)$, critical demand $D(k)$, controllable load demand $D^l(k)$, PV power $P^{PV}(k)$, their day-ahead forecasts $\hat{D}(k), \hat{P}^{PV}(k), \hat{D}^l(k)$, and previous DG states $P^{DG}(k-1), x^{DG}(k-1)$.

At each time step k , the MPC-MILP controller compute the QCC linear piecewise approximation. It then calculates and updates the forecast of critical demand, controllable load demand, and PV power, as well as determine the economic schedule. The controller implements

the first element of the control solution, and a subset of the decision vector is sent to the microgrid's local controllers:

$$\left\langle \begin{matrix} P^{DG}(k|k), x^{DG}(k|k), P^b(k|k), \\ \delta^b(k|k), P^g(k|k), \beta^l(k|k) \end{matrix} \right\rangle$$

The process is repeated in the next time step $k+1$ to ensure that the forecast is updated with the latest data and energy storage stays within the specified bounds.

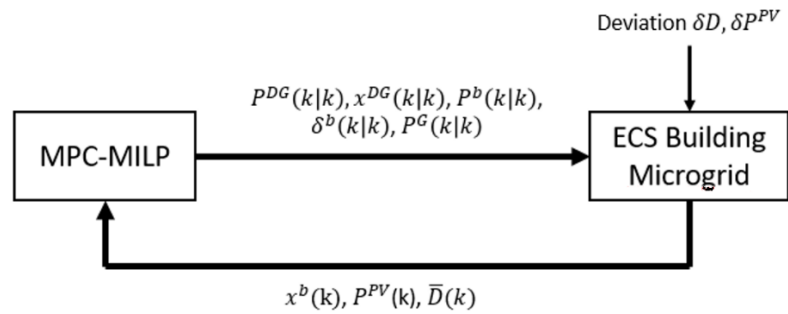


FIGURE 31: MPC-MILP control strategy

The MPC-MILP algorithm is described in Figure 31, and the flowchart of ECS microgrid's operation is shown in Figure 32.

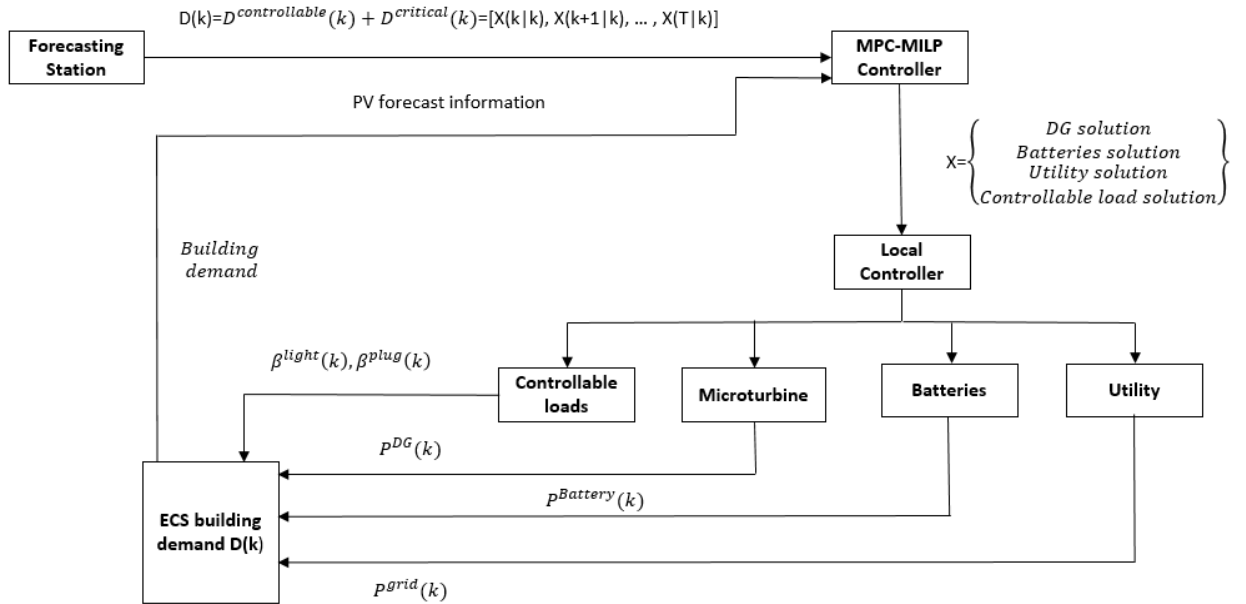


FIGURE 32: Flowchart of microgrid's operation

The optimal sequence for time step k through T calculated by the MPC-MILP control system is defined as:

$$x_{\rightarrow k}^T = [x(k|k), x(k+1|k), \dots, x(T|k)] \quad (4.23)$$

MPC-MILP controller also implements the state feedback control policy $x^b(k|k) = x^b(k)$. In summary, for each time step k , MPC-MILP determine the control solution variables subject to the following MILP problem:

$$J(k) = \min_{x_{\rightarrow k}^T} \sum_{j=0}^{T-k} \left\{ C^{OM} P^{DG}(k+j|k) + C^{min} x^{DG}(k+j|k) + \sum_{m=1}^N s_m l_m(k+j|k) + C^{SU} x^{SU}(k+j|k) + C^{SD} x^{SD}(k+j|k) + C^P(k+j) P^g(k+j|k) + \rho_c \sum_{h=1}^{N_{lights}=161} \beta_h^{lights}(k+j|k) D_h^c(k+j|k) \right\} + C^{peak} Z^g(k) \quad (4.24)$$

subject to:

QCC model, DG model

Energy storage model constraints

Storage Dynamics constraints

$$P^g(k) \leq Z^g \quad \forall k = 1, \dots, T$$

Utility grid interaction constraints

Energy balancing model constraints

Bounding constraints

$$x^b(k|k) = x^b(k)$$

Note that at each new time step k , the prediction horizon recedes, but its length stays the same. This is known as receding horizon.

CHAPTER 5

CASE STUDY: SIMULATION AND RESULTS

5.1 Proposed ECS Building Microgrid

In this thesis, we propose implementing a PV generation unit with the capacity of 105 kW (designed based on the space availability on the ECS building roof), a MT with the rated power of 65 kW, and a set of three 25.9 kWh microgrid batteries to transform the ECS building into an advanced microgrid. The building will also have a point of connection to the utility grid for backup power. The proposed ECS building microgrid is shown in Figure 33.

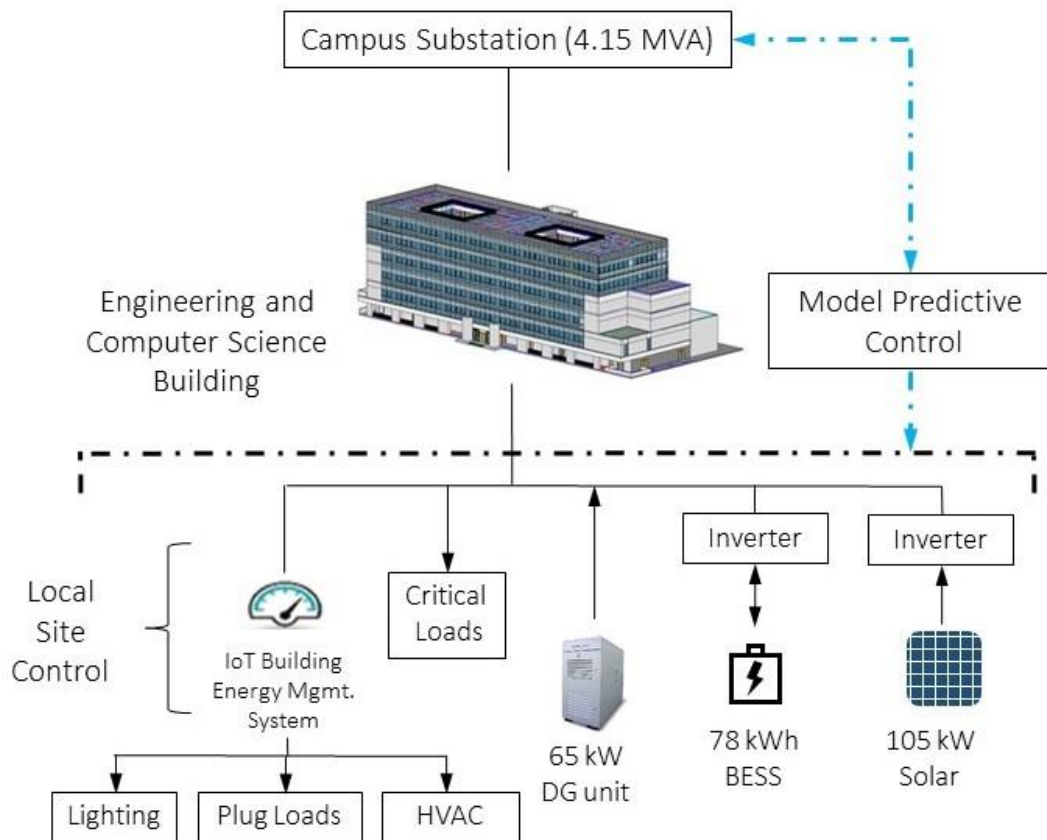


FIGURE 33: Proposed ECS building microgrid

CSULB campus is currently served by a 66kV transmission service originating from an outdoor switchyard located in the Corporation yard on the North East side of the campus.

Southern California Edison is the company who are selling power to CSULB, whereas the optimum performance of new and existing building (not only electrical, but also mechanical and plumbing) will be ensured by P2S Engineering Inc.

That 66kV service is stepped down to a 12.47kV service by using two 10/12 5mVA 66-12.47kV transformers. These transformers are served by the same high voltage breaker on the primary side. The secondary side of these transformers serves the main campus's buildings, and divided to North substation and South substation.

The North substation includes a metering section and 15kV main switchgear comprising of a 2000A main breaker and 1200A feeder breakers. There are 8 12kV feeders (numbered 1 to 8) originating from this switchgear, and they form multiple loops and serve power to various building and facilities on campus. Feeders 1 to 6 belong to the North substation, and the ECS building is supplied by Feeder 5 with installed capacity of 4.15 MVA.

As shown in Figure 33, there are two types of loads in ECS building: critical loads and controllable loads. The critical loads are loads that must be on for essential processes whenever the occupants want them to be on. The building microgrid's controllable loads such as lighting system, plug load system, and HVAC system are controlled autonomously and optimally under the IoT-based BEMS system. The BEMS system co-optimizes the IoT-based flexible lighting system with on-site resources using the proposed MPC-MILP algorithm. The PV power, building critical demand, and controllable lighting demand for the day of May 1st, 2019 along with its day-ahead forecasting are shown in Figure 34 and Figure 35.

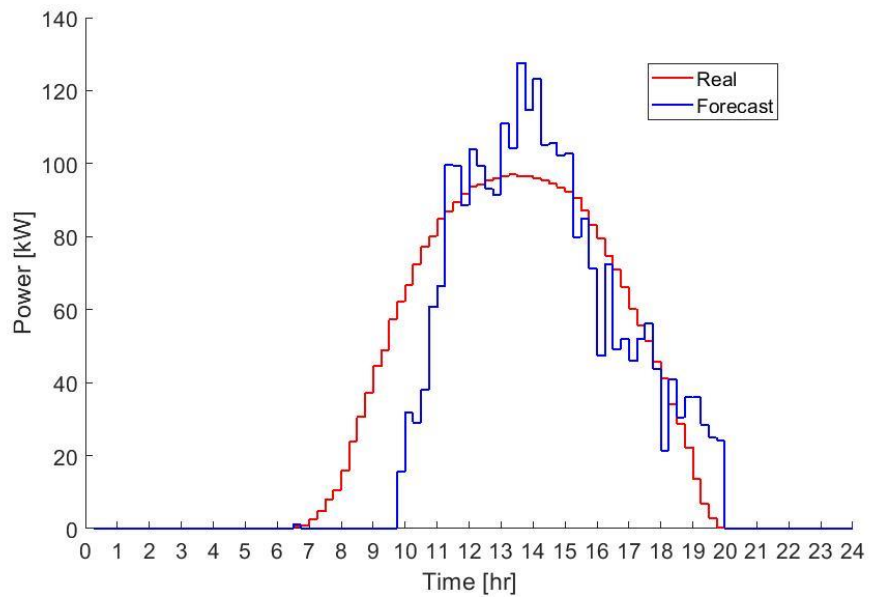


FIGURE 34: PV power forecasting

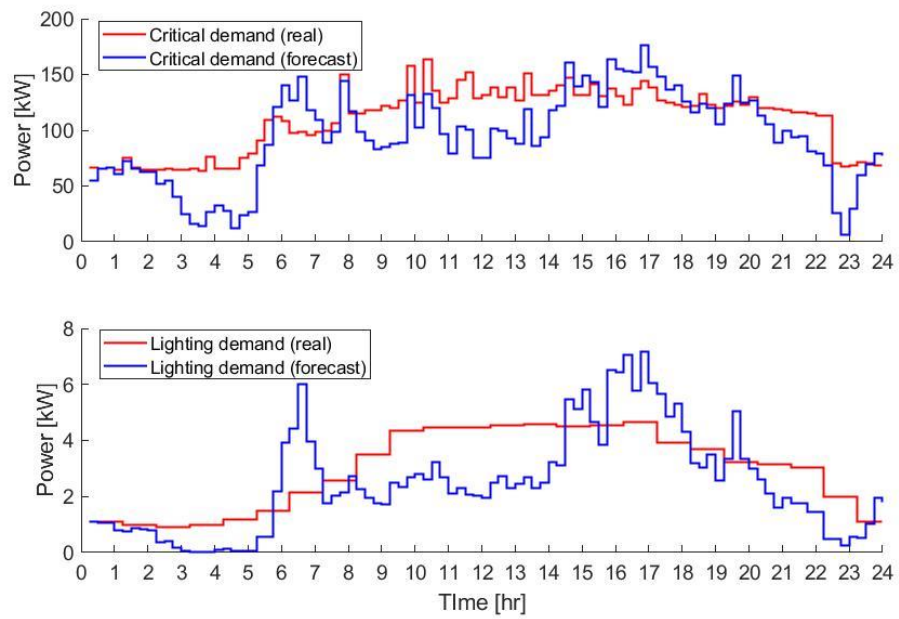


FIGURE 35: Demands forecasting

5.2 Control Strategy Setup

Four control strategies are evaluated in this study:

- All from Utility (AFU): All needed power will be supplied by the utility grid. There is neither IoT-based BEMS system nor proposed MPC-MILP control approach. The building microgrid's demand data for this control strategy is May 2015, when IoT-based BEMS has not been installed.
- AFU with IoT-based BEMS: All needed power is still supplied by the grid, but the IoT-based BEMS optimally controls the lighting, plug load, and HVAC system based on the energy, environmental and occupancy data collected by the smart sensor network. The building microgrid's demand for this control strategy is May 2019, when IoT-based BEMS has already been installed in the building.
- MPC-MILP: This is a MILP problem that is calculated at each time step k with the updated forecasts and the sampled state of the storage energy. However, this control strategy is applied to the ECS building microgrid where IoT-based BEMS does not exist. Meaning that it does not include managing and controlling the IoT-based flexible loads. This control strategy is applied to May 2015 demand data.
- MPC-MILP with IoT-based BEMS: This is the proposed control strategy of this paper. The MPC-MILP control strategy will be implemented in the IoT-based BEMS system to increase energy efficiency as well as the DR capability of the building. This control strategy is applied to May 2019 demand data.

5.3 Simulation and Results

The ECS building microgrid is simulated based on one-month operational data of May 2019. Figure 36 presents the optimal operation of the DERs and utility grid for May 1st 2019, determined by the proposed MPC approach (MPC-MILP with IoT-based BEMS), and figure 37 shows the result of MPC-MILP for May 1st, 2015.

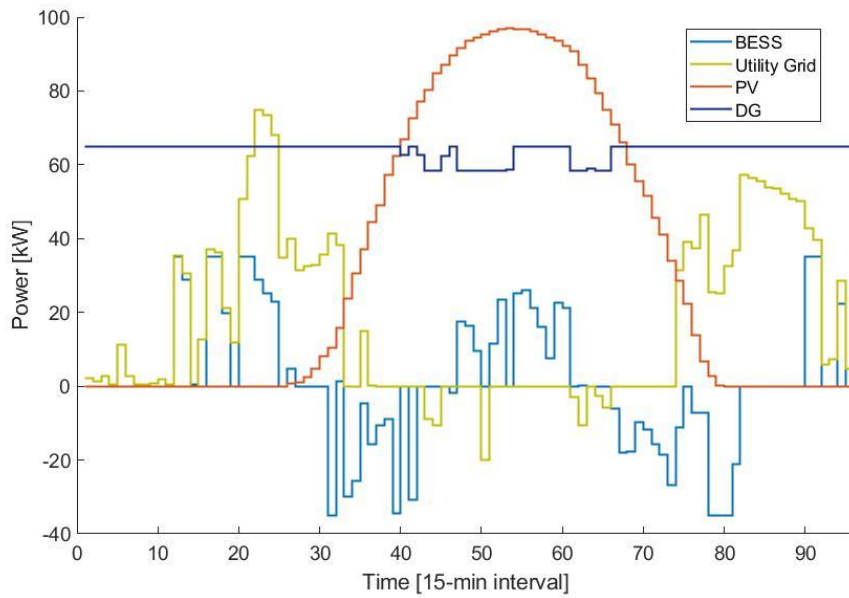


FIGURE 36: The operation of building microgrid’s components controlled by proposed MPC-MILP approach during May 1st, 2019.

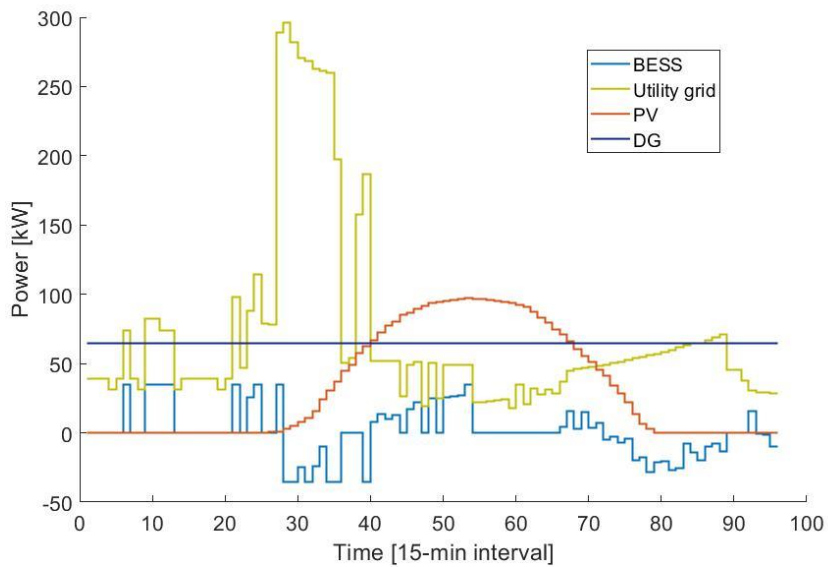


FIGURE 37: The operation of building microgrid’s components controlled by MPC-MILP approach during May 1st, 2015.

The daily operational cost of four control strategies is compared in Figure 38, and the monthly total operational cost (operational cost and peak demand cost) are provided in Table 6.

As shown in the table, the MPC-MILP with IoT-based BEMS helps the building microgrid achieve 77% savings in term of total monthly operating costs, while AFU with IoT-based BEMS and MPC-MILP provides 47% and 37% savings, respectively.

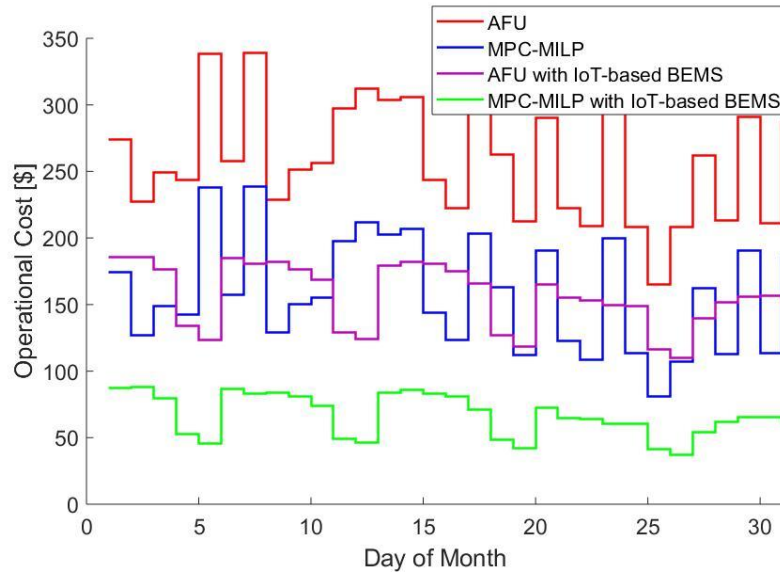


FIGURE 38: Daily operational cost comparison between four control strategies for May 2019.

We also compared the peak load reduction for four control strategies. The results show that the MPC-MILP with IoT-based BEMS provides the highest peak load reduction, 83% reduction, while the MPC-MILP strategy without load controllability only provides 34% reduction, and the AFU with IoT-based BEMS is 63%.

Strategy	Total Monthly Operational Cost (\$)	Saving (%)
All from Utility	11,989	--
AFU with IoT-based BEMS	6,277	47
MPC-MILP	7,543	37
MPC-MILP with IoT-based BEMS	2,743	77

Strategy	Monthly Peak Load (kW)	Reduction (%)
All from Utility	480	--
AFU with IoT-based BEMS	174	63
MPC-MILP	316	34
MPC-MILP with IoT-based BEMS	82	83

Table 6: Total monthly operational cost, and monthly peak demand comparison.

5.4 Unit Commitment and Economic Dispatch Discussion

The DG's unit commitment and economic dispatch relationship is described in equation X and X, where DG state and DG power need to be determined through the optimization. This process is necessary since there is cost associated with turning on or shutting down the DG. However, during our simulation, we recognized that unit commitment and economic dispatch can be considered as the same problem to solve for small scale building microgrid since DG seems not to be turned off during its operation. To examine this claim, we tested our current DG model with three cases:

- 1) Current model with no change.
- 2) Current model with $P_{min}^{DG} = P_{max}^{DG} = 65 \text{ kW}$
- 3) Current model with $x^{DG} = 1$ for all time steps.

All of three cases have been simulated with 1-day prediction horizon and 3-day prediction horizon, and cost of turning on and shutting down the DG are set to 0. Figure 39 shows the operation of DG unit for 3 mentioned cases. Results show that the DG unit kept

running constantly through the optimization process and did not turn off at any time step. Therefore, for small scale building microgrid, unit commitment problem can be merged with economic dispatch problem.

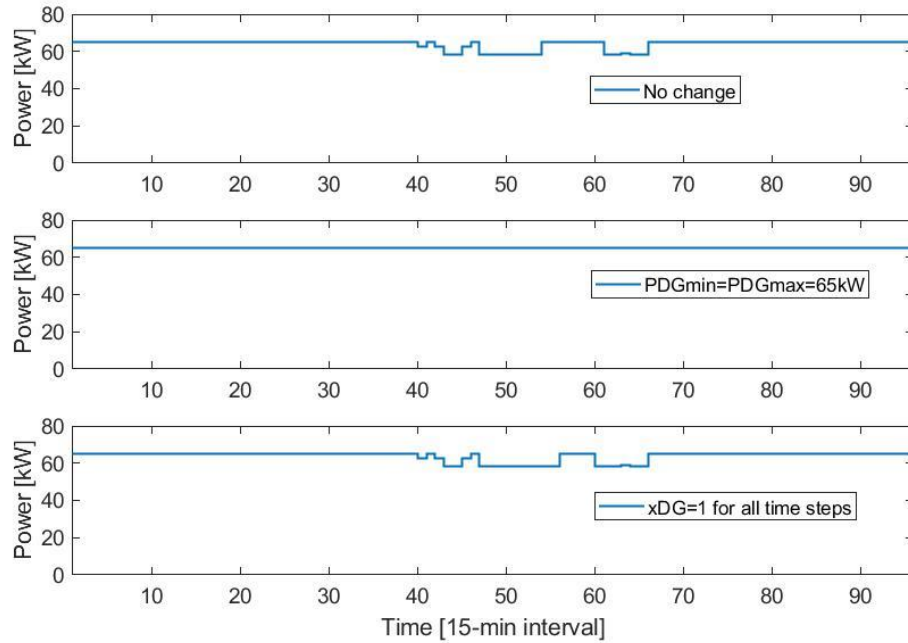


FIGURE 39: DG operation of three examining cases for May 1st, 2019.

5.5 Economic Analysis

This section aims to discuss the benefits and energy savings opportunities of implementing the IoT-based BEMS which has sensors and control across plug-in loads, lighting, and HVAC system in the ECS building, and integrating this advanced system with optimal scheduling.

5.5.1 Benefits from implementing IoT-based BEMS

As discussed previously, the IoT-based BEMS optimally controls the lighting, plug load, and HVAC system based on the energy, environmental and occupancy data collected by the smart sensor network. The proposed MPC approach receives predicted energy consumption from

the IoT-based BEMS, and performs optimal scheduling for the operation of on-site DERs and controllable lighting system.

The IoT-based EMS system also provides an opportunity for building to grid services such as DR. DR can be provided through advanced load control such as automated lighting control, automated dimming control, high granularity zonal occupancy-based lighting control, zonal occupancy-based ventilation control, automated VAV control, automated fan speed control, temporary non-essential plug load curtailment, and idle load curtailment.

The DR techniques implemented across lighting, plug-in loads and HVAC can make building load profile smoother, therefore improving grid stability and quality of service. These advanced technologies also enhance flexibility in grid management such as creating reserve capacity, increasing grid capacity through more finely tuned operations, as well as improving the grid reliability and efficiency through the energy data information exchange between assets in building and between building and the grid.

In long-term vision, it will provide cost-effective resiliency and robustness to the grid, reduce expensive investment on new generation and transmission, and enable several ancillary services, such as reducing and mitigating future costs for capacity to manage the increasing penetration of variable renewable energy sources and supporting the deployment of EVs.

Another merit of this advanced technology is the ease of deployment and integration at wide variety of existing buildings, interoperability and ability to include or work in parallel with existing and conventional energy management systems. Sensors, actuators, and other hardware are plug-and play devices, deployed without any need of hardwiring or modifications to existing circuits, thus, the fully automated IoT sensor network is deployed with minimum labor.

5.5.2 Savings and payback period

Next, we calculate the energy cost reduction of implementing and integrating the IoT-based BEMS with the proposed MPC optimal scheduling. Retail tariff, to which the CSULB campus is subject to, is SCE TOU-8-B with the average price of electricity of \$0.067/kWh, and the average energy charges and demand charges are \$7.23/kW/month, \$0.75 kVAr/kW, and \$0.34/kVAr/month.

Due to the result presented in Table 6, MPC-MILP with IoT-based BEMS can reduce 77% of the total monthly operational cost, in compared with all from utility control strategy. Considering this as the monthly average reduction, the energy cost reduction for an academic year will be $\$9,246 \times 12 = \$110,952$.

The cost of this project mainly belongs to the project equipment, installation, and maintenance. The rest of the cost is dedicated to enhancing the microgrid real-time control methodology, and energy management strategy. The microgrid equipment includes: microgrid switches, solar PV panels, battery energy storage, distributed generator, inverters, IoT communication devices, smart plug load controllers, smart sensors, smart lighting fixtures. The total project equipment and material cost (shown in Table 7), including the cost of equipment installation and maintenance, and enhanced services is estimated at \$493,157. Total estimated project cost saving per year is \$110,952. The benefit to cost ratio of the proposed project guarantees the return of investment in 4.5 years.

TABLE 7: Economic analysis of the proposed project

IoT devices, smart lights, plug load controllers (\$)	300,000
PV system (\$)	109,760
Energy storage (\$)	44,397
DG unit (\$)	39,000
Total initial invests (\$)	493,157
Total cost saving/year (\$)	110,952
Payback period (year)	4.5

CHAPTER 6

CONCLUSION

This thesis presents an economic scheduling framework for building microgrids with IoT-based controllable loads. The load controllability, curtailment level constraints, and curtailment penalty have been implemented in the modeling and optimization of the building microgrid. The proposed approach has been investigated on the Engineering and Computer Science (ECS) building microgrid at the CSULB campus. The simulation results show that the proposed MPC-MILP method with IoT-based load controllability leads to superior energy costs saving and peak load reduction. They also show that in small scale building microgrid, unit commitment and economic dispatch can be considered as the same problem to solve since DG seems not to be turned off during its operation.

In addition, during the smart building microgrid design process, we have discovered that only 24% of total number of building's outlet should be replaced by smart plug controllers to achieve maximum energy efficiency and demand response capabilities on plug-in loads. The benefits and economic analysis of implementing the advanced energy efficiency controllable loads and integrating them with proposed control platform of building micro-grid also have been conducted and presented.

Many existing building owners are reluctant to take on brand-new technologies or upgrades due to the need for additional in-house technical personnel and expertise. One of the goals of this project is to remove those barriers to achieve widespread deployment of state-of-the-art energy management technologies in academic buildings by addressing the specific energy needs of such buildings. The successful demonstration of advanced building energy efficiency and DR capability paves the way for future deployments in other academic buildings. This

deployment project can make radical improvements to the carbon footprint, electricity use, deployment infrastructure and demand response scaling.

Future research endeavors include applying machine learning algorithm for demands forecasting, developing a mathematical model for the penalty cost curve of controllable load curtailment, and extending the MPCMILP approach to the IoT network of the HVAC system to increase overall energy efficiency and demand response capability. The HVAC system can be controlled using occupancy data to optimally adjust air handlers and air volume at different zones. In addition, by applying machine learning methods we can predict the behavior of occupants. This information can be used for prior scheduling of the HVAC system for pre-cooling or pre-heating the zones, which can result in significant energy costs savings.

APPENDIX A

MATLAB CODE OF MPC-MILP CONTROLLER (1-day prediction horizon)

Matlab code of the proposed MPC-MILP controller

```

function [xPDG1,xDG1,xSU1,xSD1,xBeta1,xPb1,xdeltb1,xPgrid1,xdeltg1,...
        xBeta_lighting1, lighting_controllable_demand1,...
        Lighting_penalty] = ...
        MPC_MILP(xb_measured_state,Pres_measured_state,D_measured_state,...
        Time_Step,Prev_PDG_State,Prev_xDG_State,controllableLoad,demand,...
        gridPurchasing,gridSelling,RES_Power,rand_variable_demand,...
        rand_variable_RES,light_profile)    %#codegen

samp_per = 0.25;    % sampling period [hrs] (ex. 15 min => 0.25)

Ninitial = 24/samp_per; % Sample periods for the day
N = Ninitial; %fixed prediction horizon (24-hour=96)

% Sampling period for Simulink purposes
delta_t = (samp_per)*60*60; % sampling period for 24 hr [sec.]

%%%%%%%%%%%%%%%%%%%%%%%%%%%%%%%%%%%%%%%%%%%%%%%%%%%%%%%%%%%%%%%%%%%%%%%%
%%%%%%%% Distributed Generator: Microturbine: Capstone C65 %%%%
%%%%%%%%%%%%%%%%%%%%%%%%%%%%%%%%%%%%%%%%%%%%%%%%%%%%%%%%%%%%%%%%%%%%%%%%

% DG unit power parameters
PDG_min = 0;    % minimum power output for the DG unit [kW]
PDG_max = 65.0; % maximum power output for the DG unit [kW]

% DG Cost parameters
cStartUp = 0.0000;    % Startup cost for DG [$]
cShutdown = 0.0000;    % Shutdown cost for DG [$]
MaintOppCoeff = 0.00325; % [$/kW] (see pg. 178 of notebook)

RRu = 360;    % Ramp rate up limit [kW/hr] (MUST be positive)
RRu = RRu*samp_per;

RRd = 360;    % Ramp rate down limit [kW/hr] (MUST be positive)
RRd = RRd*samp_per;

%%%%%%%%%%%%%%%%%%%%%%%%%%%%%%%%%%%%%%%%%%%%%%%%%%%%%%%%%%%%%%%%%%%%%%%%
%%%%%%%% Microgrid Battery: Aspen 48M-25.9 Battery %%%%%%%%%
%%%%%%%%%%%%%%%%%%%%%%%%%%%%%%%%%%%%%%%%%%%%%%%%%%%%%%%%%%%%%%%%%%%%%%%%
% Note: We will be placing three (3) of these batteries in parallel. Thus,
% we will triple the capacity and power output limit.

% Energy storage global parameters
xbinitial = 5.0; % Initial energy state of the storage device (at t = 0)
                % [kWh]. Thus, xb(1) = xbinitial;
xbfinal = 5.0; % The starting energy state of the storage device for
                % tomorrow [kWh]. Thus, xb(N+1) = xbfinal;
xbStorageMin = 5.0; % Minimum energy storage for our battery/UC [kWh]
                % this is if you don't want SOC below a certain level
                % Note: this value must be non-negative

```

```

xbStorageMax = 3*25.9; % Maximum energy storage for our battery/UC [kWh]
Pb_chg_dchg_lim = 3*11.7;% Max power rate storage can CHARGE/DISCHARGE [kW]
Cb = Pb_chg_dchg_lim; % *NOTE*: Keep track of where the negative is
                        % implemented, here or in the "Lower and upper
                        % bound constraints" segment.
eff_c = 0.95; % Charging efficiency of en. storage + pwr electronics.
           % with 0 <= eff_c <= 1; 1 means no power loss.
eff_d = 0.95; % Discharging efficiency of en. storage + pwr electronics.
           % with 0 <= eff_d <= 1; 1 means no power loss.
xsb = 0.0027; % const. stored energy degradation in sampling interval [kWh]

```

```

%%%%%%%%%%%%%%%%%%%%%%%%%%%%%%%%%%%%%%%%%%%%%%%%%%%%%%%%%%%%%%%%%%%%%%%%
%%%%%%%% Utility Grid: Provider: Southern California Edison %%%%%%%%%
%%%%%%%%%%%%%%%%%%%%%%%%%%%%%%%%%%%%%%%%%%%%%%%%%%%%%%%%%%%%%%%%%%%%%%%%

```

```

% Utility Grid parameters
Tg = 2000; % Maximum interconnected power flow limit [kW]

```

```

c_peak = 6.56/31; % Peak demand cost coefficient [$/kW]

```

```

%penalty for controllable lighting load

```

```

rho_c_lighting = 0.067;

```

```

%% Extrinsic Declarations and Nullcopies, etc.
% As required by the MATLAB Function block, you must declare certain
% functions as extrinsic, and use nullcopy accordingly.

```

```

coder.extrinsic('cplexmilp');
coder.extrinsic('round');
coder.extrinsic('abs');

```

```

% preinitializing for variables dependant on extrinsic funtions

```

```

xPDG = coder.nullcopy(zeros(N,1)); %#ok<NASGU> Ignore this warning
xLDG = coder.nullcopy(zeros(10*N,1)); %#ok<NASGU> Ignore this warning
xDG = coder.nullcopy(zeros(N,1)); %#ok<NASGU> Ignore this warning
xSU = coder.nullcopy(zeros(N,1)); %#ok<NASGU> Ignore this warning
xSD = coder.nullcopy(zeros(N,1)); %#ok<NASGU> Ignore this warning
xBeta = coder.nullcopy(zeros(N,1)); %#ok<NASGU> Ignore this warning
xb = coder.nullcopy(zeros(N,1)); %#ok<NASGU> Ignore this warning
xPb = coder.nullcopy(zeros(N,1)); %#ok<NASGU> Ignore this warning
xdeltb = coder.nullcopy(zeros(N,1)); %#ok<NASGU> Ignore this warning
xzb = coder.nullcopy(zeros(N,1)); %#ok<NASGU> Ignore this warning
xPgrid = coder.nullcopy(zeros(N,1)); %#ok<NASGU> Ignore this warning
xdeltg = coder.nullcopy(zeros(N,1)); %#ok<NASGU> Ignore this warning
xCg = coder.nullcopy(zeros(N,1)); %#ok<NASGU> Ignore this warning
xBeta_lighting = coder.nullcopy(zeros(161,N)); %#ok<NASGU> Ignore this
warning
%xBeta_plug = coder.nullcopy(zeros(201,N)); %#ok<NASGU> Ignore this warning
xPDG1 = coder.nullcopy(zeros(size(1))); %#ok<NASGU> Ignore this warning

```

```

xDG1      = coder.nullcopy(zeros(size(1))); %#ok<NASGU> Ignore this warning
xSU1      = coder.nullcopy(zeros(size(1))); %#ok<NASGU> Ignore this warning
xSD1      = coder.nullcopy(zeros(size(1))); %#ok<NASGU> Ignore this warning
xBeta1    = coder.nullcopy(zeros(size(1))); %#ok<NASGU> Ignore this warning
xPb1      = coder.nullcopy(zeros(size(1))); %#ok<NASGU> Ignore this warning
xdeltb1   = coder.nullcopy(zeros(size(1))); %#ok<NASGU> Ignore this warning
xPgrid1   = coder.nullcopy(zeros(size(1))); %#ok<NASGU> Ignore this warning
xdeltg1   = coder.nullcopy(zeros(size(1))); %#ok<NASGU> Ignore this warning
xBeta_lighting1 = coder.nullcopy(zeros(161,1)); %#ok<NASGU> Ignore this
warning
%xBeta_plug1 = coder.nullcopy(zeros(201,1)); %#ok<NASGU> Ignore this warning
%fvallLP= coder.nullcopy(zeros(1,1));
%Plug_penalty=coder.nullcopy(zeros(1,1));
Lighting_penalty=coder.nullcopy(zeros(1,1));
%% Piecewise Linear Approx. of DG unit's Fuel Quadratic Cost Curve (QCC)
% Extracting a linear cost function from the Capstone C65 from the user's
% manual.

% DG unit power parameters
PDG_min = 0;      % minimum power output for the DG unit [kW]
PDG_max = 65.0;  % maximum power output for the DG unit [kW]

% Solution: C(PDG) -0.0001*PDG^2 + 0.0294*PDG + 0.2410
% a1,a2,a3 of Capstone C65: % See CapStone_C65_Fuel_Cost_Curve_Data.m
a1 = -0.0001;
a2 = 0.0294;
a3 = 0.2410;

% To plot QCC
pp = linspace(0,PDG_max*1.20,150);
QCC = a1*pp.^2 + a2*pp + a3; %#ok<NASGU> % Quadratic Cost Curve (QCC)
QCC_coeffs = [a1,a2,a3];

Cmin = polyval(QCC_coeffs,PDG_min); % QCC(Pmin)

% Initialize Linear Approx. Parameters
SG = 10;      % Number to segments in your pcw linear approx.
P_DGm0 = PDG_min;
P_DGm = zeros(SG,1); % initializing PDGmax

for ii = 1:SG
    P_DGm(ii) = PDG_min + (PDG_max - PDG_min).*(ii/SG);% The partitions pts
end
P_DGm = [P_DGm0;P_DGm]; % 11 elements

% Slope Implementation
S = zeros(SG,1); % Initialize S(k)

for ii = 1:SG
    S(ii) = ...
        (polyval(QCC_coeffs,P_DGm(ii+1)) - polyval(QCC_coeffs,P_DGm(ii)))/...
        (P_DGm(ii+1) - P_DGm(ii));
end

```

```

%% % LDG1, LDG2, ... Zero matrices

LDGZeros = zeros(N,SG*N); % I used this instead of the commented out since
                        % I was getting a loop-allocation error.

%% Forecast Modeling w/ correlation (Model from Gan: dlc_eenergy.pdf)
%% This code works for the shrinking horizon MPC-MILP code only
% This file will model a forecast for critical load, controllable loads and
%RES power at a time step k. This is set to be implemented in both MILP and
%MPC-MILP Control Systems. This model was primarily taken from "Real-Time
%Deferrable Load Control: Handling the Uncertainties of Renewable Generation"
%by Gan

RES_Power_kk = RES_Power;
demand_kk = demand;

error_cap_Horizon = 20;

e_RES = 10.23*rand_variable_RES;
e_demand = 10.23*rand_variable_demand;
%e_controllable_load=0.005*rand_variable_demand;
e_controllable_load=0.02*rand_variable_demand;

filter_type = 1;

delta_filt = 12; % Choose a value

a_filt = 0.5;

%%%%%%%%%%%%%%%%%%%%%%%%%%%%%%%%%%%%%%%%%%%%%%%%%%%%%%%%%%%%%%%%%%%%%%%%
%%%%%%%%%%%%%%%%%%%%%%%%%%%%%%%%%%%%%%%%%%%%%%%%%%%%%%%%%%%%%%%%%%%%%%%% RES Power %%%%%%%%%%%%%%%%%%%%%%%%%%%%%%%%%%%%%%%%%%%%%%%%%%%%%%%%%%%%%%%%%%%%%%%%%
%%%%%%%%%%%%%%%%%%%%%%%%%%%%%%%%%%%%%%%%%%%%%%%%%%%%%%%%%%%%%%%%%%%%%%%%

RES_Power_hat = zeros(1,N);
b_RES = zeros(1,96);

% This is for b(tau)
count = 1;
for ii = Time_Step:(96-1+Time_Step)
    b_RES(count) = RES_Power_kk(ii) + deviation(e_RES,filter_type,...
                                                delta_filt,a_filt,...
                                                1,ii);
    count = count + 1;
end

% This is the h-filter
E_RES_Power = zeros(1,N);

if error_cap_Horizon <= N
    for ii = 1:(error_cap_Horizon)
        E_RES_Power(ii) = 1 - (ii-1)/error_cap_Horizon;
    end
end

```

```

    end
else
    for ii = 1:N
        E_RES_Power(ii) = 1 - (ii-1)/error_cap_Horizon;
    end
end

% This is for RES solar
count = 1;
for ii = 1:96
    RES_Power_hat(count) = ...
        b_RES(ii) - E_RES_Power(count)*deviation(e_RES,filter_type,...
                                                    delta_filt,a_filt,...
                                                    1,ii);

    count = count + 1;
end

% Extra tailoring
for ii = 1:N
    if RES_Power_hat(ii) < 0
        RES_Power_hat(ii) = 0;
    end
end

RES_Power_hat(1) = Pres_measured_state;
RES_Power_hat=RES_Power_hat';
%%%%%%%%%%%%%%%%%%%%%%%%%%%%%%%%%%%%%%%%%%%%%%%%%%%%%%%%%%%%%%%%%%%%%%%%
%%%%%%%%%%%%%%%%%%%%%%%%%%%%%%%%%%%%%%%%%%%%%%%%%%%%%%%%%%%%%%%%%%%%%%%% Critical Demand %%%%%%%%%%
%%%%%%%%%%%%%%%%%%%%%%%%%%%%%%%%%%%%%%%%%%%%%%%%%%%%%%%%%%%%%%%%%%%%%%%%

demand_hat = zeros(1,N);
b_demand = zeros(1,96);

% This is for b(tau)
count = 1;
for ii = Time_Step:(96-1+Time_Step)
    b_demand(count) = demand_kk(ii) + deviation(e_demand,filter_type,...
                                                    delta_filt,a_filt,...
                                                    1,ii);

    count = count + 1;
end

% This is the h-filter
E_demand = zeros(1,N);

if error_cap_Horizon <= N
    for ii = 1:(error_cap_Horizon)
        E_demand(ii) = 1 - (ii-1)/error_cap_Horizon;
    end
else
    for ii = 1:N
        E_demand(ii) = 1 - (ii-1)/error_cap_Horizon;
    end
end

```

```

end

% This is for demand
count = 1;
for ii = 1:96
    demand_hat(count) = ...
        b_demand(ii) - E_demand(count)*deviation(e_demand,filter_type,...
                                                    delta_filt,a_filt,...
                                                    1,ii);

    count = count + 1;
end

% Extra tailoring
for ii = 1:N
    if demand_hat(ii) < 0
        demand_hat(ii) = 0;
    end
end

demand_hat(1) = D_measured_state;
demand_hat=demand_hat';

%%%%%%%%%%%%%%%%%%%%%%%%%%%%%%%%%%%%%%%%%%%%%%%%%%%%%%%%%%%%%%%%%%%%%%%%
%%% Controllable Lighting Demand %%%%%%%%%
%%%%%%%%%%%%%%%%%%%%%%%%%%%%%%%%%%%%%%%%%%%%%%%%%%%%%%%%%%%%%%%%%%%%%%%%
light_demand_hat = zeros(161,N);

for jj=1:161
    b_demand = zeros(1,96);
    light_demand_kk=light_profile(jj,:);
    % This is for b(tau)
    count = 1;
    for ii = Time_Step:(96-1+Time_Step)
        b_demand(count) = light_demand_kk(ii) +
            deviation(e_controllable_load,filter_type,...
                    delta_filt,a_filt,...
                    1,ii);

        count = count + 1;
    end

% This is the h-filter
E_demand = zeros(1,N);

if error_cap_Horizon <= N
    for ii = 1:(error_cap_Horizon)
        E_demand(ii) = 1 - (ii-1)/error_cap_Horizon;
    end
else
    for ii = 1:N
        E_demand(ii) = 1 - (ii-1)/error_cap_Horizon;
    end
end

% This is for controllable lighting demand
count = 1;

```

```

for ii = 1:96
    light_demand_hat(jj,count) = ...
        b_demand(ii) -
E_demand(count)*deviation(e_controllable_load,filter_type,...
                            delta_filt,a_filt,...
                            1,ii);

    count = count + 1;
end

% Extra tailoring
for ii = 1:N
    if light_demand_hat(jj,ii) < 0
        light_demand_hat(jj,ii) = 0;
    end
end

light_demand_hat(jj,1) = light_profile(jj,Time_Step);
end
total_light_demand_hat=zeros(N,1);
total_light_demand_hat=(sum(light_demand_hat))';

controllableLoad_k = zeros(N,1);
gridPurchasing_k = zeros(N,1);
gridSelling_k = zeros(N,1);

% controllableLoad
count = 1;
for ii = Time_Step:Ninitial
    controllableLoad_k(count) = controllableLoad(ii);
    count = count + 1;
end

% gridPurchasing
gridPurchasing_kk=gridPurchasing;
count = 1;
for ii = Time_Step:(96-1+Time_Step)
    gridPurchasing_k(count) = gridPurchasing_kk(ii);
    count = count + 1;
end

% gridSelling
gridSelling_kk=gridSelling;
count = 1;
for ii = Time_Step:(96-1+Time_Step)
    gridSelling_k(count) = gridSelling_kk(ii);
    count = count + 1;
end

% PDG costs
PDG_Cost = MaintOppCoeff*ones(N,1);

% LDG1, LDG2, ... costs
LDG_Cost = samp_per*ones(SG*N,1);

```

```

for ii = 1:SG
    if ii == 1
        LDG_Cost = samp_per*S(ii)*ones(N,1);
    else
        LDG_Cost = [LDG_Cost;samp_per*S(ii)*ones(N,1)];
    end
end

% xDG costs
xDG_Cost = samp_per*Cmin*ones(N,1);

% xSU cost vector
SUcost = ones(N,1)*cStartUp;

% xSD cost vector
SDcost = ones(N,1)*cShutdown;

% Beta cost vector
betaCost = zeros(N,1);

% xb cost vector
xbCost = zeros(N,1);

% Pb cost vector
PbCost = zeros(N,1);

% deltb cost vector
deltbCost = zeros(N,1);

% zb cost vector
zbCost = zeros(N,1);

% Pgrid cost vector
PgCost = zeros(N,1);

% deltg cost vector
deltgCost = zeros(N,1);

CgCost = ones(N,1);

% Zg cost vector
ZgCost = c_peak*1;

% Beta_lighting cost vector
Beta_lighting_Cost = zeros(161*N,1);

for ii = 1:161
    Beta_lighting = zeros(N,1);
    Beta_lighting = rho_c_lighting*(CntlLoad_lighting(ii,Time_Step:(96-
1+Time_Step)))';
    Beta_lighting_Cost(N*(ii-1)+1:N*ii) = Beta_lighting;
end

costs = [PDG_Cost;LDG_Cost;xDG_Cost;SUcost;SDcost;betaCost;xbCost;...

```

```

        PbCost;deltbCost;zbCost;PgCost;deltgCost;CgCost;ZgCost;...
        Beta_lighting_Cost];

Acomm1 = [-eye(N),LDGZeros,PDG_min*eye(N),zeros(N),zeros(N),zeros(N),...
          zeros(N),zeros(N),zeros(N),zeros(N),zeros(N),zeros(N),...
          zeros(N),zeros(N,1),zeros(N,161*N)];
Acomm2 = [eye(N),LDGZeros,-PDG_max*eye(N),zeros(N),zeros(N),zeros(N),...
          zeros(N),zeros(N),zeros(N),zeros(N),zeros(N),zeros(N),...
          zeros(N),zeros(N,1),zeros(N,161*N)];

Bcomm1 = zeros(N,1);
Bcomm2 = zeros(N,1);

A = [Acomm1;Acomm2];
coder.varsize('A'); %supporting variable-size data
B = [Bcomm1;Bcomm2];

kk = 1; % Initialize counter
for ii = 1:SG
    Alk=[];
    Alk = zeros(N); % PDG
    for jj = 1:SG
        if jj == kk
            Alk = [Alk, eye(N)]; %#ok<AGROW> Ignore warning
        else
            Alk = [Alk, zeros(N)]; %#ok<AGROW> Ignore warning
        end
    end
    Alk = [Alk, -(P_DGm(ii+1) - P_DGm(ii)).*eye(N),zeros(N),zeros(N),...
            zeros(N),zeros(N),zeros(N),zeros(N),zeros(N),zeros(N),...
            zeros(N),zeros(N),zeros(N,1),zeros(N,161*N)]; %#ok<AGROW> Ignore
    kk = kk + 1;
    A = [A;Alk]; %#ok<AGROW> Ignore warning
end

Blk = zeros(SG*N,1);

B = [B;Blk];

su = diag(-ones(1,N-1),-1) + eye(N);

% zeros matrixs to null shutdown, xb, Pb, grid to not get mixed in all this
% StUp constraints
Astart1 = [zeros(N),LDGZeros,su,-eye(N),zeros(N),zeros(N),zeros(N),...
           zeros(N),zeros(N),zeros(N),zeros(N),zeros(N),zeros(N),...
           zeros(N,1),zeros(N,161*N)];

Bstart1 = zeros(N,1);
A = [A;Astart1];
B = [B;Bstart1];

sd = diag(ones(1,N-1),-1) - eye(N);

```

```

Astart2 = [zeros(N), LDGZeros, sd, zeros(N), -eye(N), zeros(N), zeros(N), ...
           zeros(N), zeros(N), zeros(N), zeros(N), zeros(N), zeros(N), ...
           zeros(N,1), zeros(N,161*N)];

Bstart2 = zeros(N,1);
A = [A;Astart2];
B = [B;Bstart2];

Aru = diag(-ones(1,N)) + diag(ones(1,N-1),1);
Aru(N,N) = 0;

Aru = [Aru, LDGZeros, zeros(N), zeros(N), zeros(N), zeros(N), zeros(N), ...
       zeros(N), zeros(N), zeros(N), zeros(N), zeros(N), zeros(N), ...
       zeros(N,1), zeros(N,161*N)];

A = [A;Aru];

Bru = RRu.*ones(N,1);
B = [B;Bru];

%% DG Power ramp-down rate constraints
% Very similar to ramp-up limit , just flip the signs of the decision
% variables

% The decision vector as of 6/7/18:
% % x = [PDG lk xDG xSU xSD NULL xb Pb deltb zb Pg deltg Cg Zg
Beta_lighting_(1-4) Beta_plug_(1-4)]

Ard = diag(ones(1,N)) + diag(-ones(1,N-1),1);
Ard(N,N) = 0;

Ard = [Ard, LDGZeros, zeros(N), zeros(N), zeros(N), zeros(N), zeros(N), ...
       zeros(N), zeros(N), zeros(N), zeros(N), zeros(N), zeros(N), ...
       zeros(N,1), zeros(N,161*N)];

A = [A;Ard];

Brd = RRd.*ones(N,1);
B = [B;Brd];

sxb = -eye(N) + diag(ones(1,N-1),1);

Astdy = [zeros(N), LDGZeros, zeros(N), zeros(N), zeros(N), zeros(N), sxb, ...
         -samp_per*(1/eff_d)*eye(N), zeros(N), -samp_per*(eff_c-(1/eff_d)) ...
         *eye(N), zeros(N), zeros(N), zeros(N), zeros(N), zeros(N,1), zeros(N,161*N)];

Bstdy = -samp_per*sxb.*ones(N,1);
Bstdy(N) = -xbfinal - (samp_per*sxb); % Does this need samp_per?

Aeq = Astdy;
Beq = Bstdy;

```

```

% Different Charging/Discharging Efficiencies for Storage Unit Dynamics

% (5a) Inequality (see pg. 112 of Notebook)
Ab1 = [zeros(N), LDGZeros, zeros(N), zeros(N), zeros(N), zeros(N), zeros(N), ...
       -eye(N), Cb*eye(N), zeros(N), zeros(N), zeros(N), zeros(N), ...
       zeros(N,1), zeros(N,161*N)];
Bb1 = Cb*ones(N,1);

% (5b) Inequality
Ab2 = [zeros(N), LDGZeros, zeros(N), zeros(N), zeros(N), zeros(N), zeros(N), ...
       eye(N), -(Cb+eps)*eye(N), zeros(N), zeros(N), zeros(N), ...
       zeros(N), zeros(N,1), zeros(N,161*N)];
Bb2 = eps*ones(N,1);

% (5c) Inequality
Ab3 = [zeros(N), LDGZeros, zeros(N), zeros(N), zeros(N), zeros(N), zeros(N), ...
       -eye(N), Cb*eye(N), eye(N), zeros(N), zeros(N), zeros(N), ...
       zeros(N,1), zeros(N,161*N)];
Bb3 = Cb*ones(N,1);

% (5d) Inequality
Ab4 = [zeros(N), LDGZeros, zeros(N), zeros(N), zeros(N), zeros(N), zeros(N), ...
       eye(N), Cb*eye(N), -eye(N), zeros(N), zeros(N), zeros(N), ...
       zeros(N,1), zeros(N,161*N)];
Bb4 = Cb*ones(N,1);

% (5e) Inequality
Ab5 = [zeros(N), LDGZeros, zeros(N), zeros(N), zeros(N), zeros(N), zeros(N), ...
       zeros(N), -Cb*eye(N), eye(N), zeros(N), zeros(N), zeros(N), ...
       zeros(N,1), zeros(N,161*N)];
Bb5 = zeros(N,1);

% (5f) Inequality
Ab6 = [zeros(N), LDGZeros, zeros(N), zeros(N), zeros(N), zeros(N), zeros(N), ...
       zeros(N), -Cb*eye(N), -eye(N), zeros(N), zeros(N), zeros(N), ...
       zeros(N,1), zeros(N,161*N)];
Bb6 = zeros(N,1);

% Inequality Concatenation
A = [A;Ab1;Ab2;Ab3;Ab4;Ab5;Ab6];
B = [B;Bb1;Bb2;Bb3;Bb4;Bb5;Bb6];

ADGeq = eye(N); % PDG

for ii = 1:SG
    ADGeq = [ADGeq,-eye(N)]; %#ok<AGROW> Ignore warning
end

ADGeq = [ADGeq,-PDG_min*eye(N), zeros(N), zeros(N), zeros(N), zeros(N), ...
        zeros(N), zeros(N), zeros(N), zeros(N), zeros(N), zeros(N), ...
        zeros(N,1), zeros(N,161*N)];

```

```

Aeq = [Aeq;ADGeq];

BDGeq = zeros(N,1);
Beq = [Beq;BDGeq];

AeqpwrBeta_lighting = zeros(N,161*N);

AeqpwrBeta_lighting_row = zeros(N,N);

for jj = 1:161
    k=Time_Step;
    %k=1; %fixed 24-hour prediction horizon
    for ii = 1:N

        AeqpwrBeta_lighting_row(ii,ii) = CntlLoad_lighting(jj,k);
        k=k+1;
    end

    AeqpwrBeta_lighting(1:N,N*(jj-1)+1:N*jj) = AeqpwrBeta_lighting_row;

end
% Power balance equality for controllable plug loads
Aeqpwr = [eye(N),LDGZeros,zeros(N),zeros(N),zeros(N),zeros(N),...
          zeros(N),-eye(N),zeros(N),zeros(N),eye(N),zeros(N),zeros(N),...
          zeros(N,1),AeqpwrBeta_lighting];
Aeq = [Aeq;Aeqpwr];

% beqpwr = demand + CntlLoad_lighting_1 + CntlLoad_lighting_2 +
CntlLoad_lighting_3 + CntlLoad_lighting_4 +...
% CntlLoad_plug_1 + CntlLoad_plug_2 + CntlLoad_plug_3 + CntlLoad_plug_4 -
RES_Power_k;
% beqpwr = demand_hat + total_light_demand_hat + total_plug_demand_hat -
RES_Power_hat;
beqpwr = demand_hat + total_light_demand_hat - RES_Power_hat;
Beq = [Beq;beqpwr];

%% Buying & Selling Energy Dynamics for Utility Grid
% This segment is to implement the dynamics of having the option to
% purchase and sell energy to/from the main grid. More info on this is
% found in MPC by Parisio, [36] in Parisio. From (10) in MPC, Parisio:
%  $Eg1 \cdot \text{deltg} + Eg2 \cdot Cg \leq Eg3 \cdot Pg + Eg4$ 

% The decision vector as of 6/7/18:
% % x = [PDG lk xDG xSU xSD NULL xb Pb deltb zb Pg deltg Cg Zg
Beta_lighting_(1-4) Beta_plug_(1-4)]

% This is for  $Mg = \max(cP, cS) \cdot Tg$ ;
AMg = zeros(N);
for ii = 1:N
    AMg(ii,ii) = max([gridPurchasing_k(ii),gridSelling_k(ii)]) * Tg;
end

BMg = zeros(N,1);

```

```

for ii = 1:N
    BMg(ii) = max([gridPurchasing_k(ii),gridSelling_k(ii)])*Tg;
end

% (4a) Inequality (see pg. 104 of Notebook)
Ag1 = [zeros(N),LDGZeros,zeros(N),zeros(N),zeros(N),zeros(N),zeros(N),...
        zeros(N),zeros(N),zeros(N),-eye(N),Tg*eye(N),zeros(N),...
        zeros(N,1),zeros(N,161*N)];
Bg1 = Tg*ones(N,1);

% (4b) Inequality
Ag2 = [zeros(N),LDGZeros,zeros(N),zeros(N),zeros(N),zeros(N),zeros(N),...
        zeros(N),zeros(N),zeros(N),eye(N),-(Tg+eps)*eye(N),zeros(N),...
        zeros(N,1),zeros(N,161*N)];
Bg2 = -eps*ones(N,1);

% (4c) Inequality
Ag3 = [zeros(N),LDGZeros,zeros(N),zeros(N),zeros(N),zeros(N),zeros(N),...
        zeros(N),zeros(N),zeros(N),-diag(gridPurchasing_k),AMg,eye(N),...
        zeros(N,1),zeros(N,161*N)];
Bg3 = BMg;

% (4d) Inequality
Ag4 = [zeros(N),LDGZeros,zeros(N),zeros(N),zeros(N),zeros(N),zeros(N),...
        zeros(N),zeros(N),zeros(N),diag(gridPurchasing_k),AMg,-eye(N),...
        zeros(N,1),zeros(N,161*N)];
Bg4 = BMg;

% (4e) Inequality
Ag5 = [zeros(N),LDGZeros,zeros(N),zeros(N),zeros(N),zeros(N),zeros(N),...
        zeros(N),zeros(N),zeros(N),-diag(gridSelling_k),-AMg,eye(N),...
        zeros(N,1),zeros(N,161*N)];
Bg5 = zeros(N,1);

% (4f) Inequality
Ag6 = [zeros(N),LDGZeros,zeros(N),zeros(N),zeros(N),zeros(N),zeros(N),...
        zeros(N),zeros(N),zeros(N),diag(gridSelling_k),-AMg,-eye(N),...
        zeros(N,1),zeros(N,161*N)];
Bg6 = zeros(N,1);

% Inequality Concatenation
A = [A;Ag1;Ag2;Ag3;Ag4;Ag5;Ag6];
B = [B;Bg1;Bg2;Bg3;Bg4;Bg5;Bg6];

Ap1 = [zeros(N),LDGZeros,zeros(N),zeros(N),zeros(N),zeros(N),zeros(N),...
        zeros(N),zeros(N),zeros(N),eye(N),zeros(N),zeros(N),-ones(N,1),...
        zeros(N,161*N)];
Bp1 = zeros(N,1);

% Inequality Concatenation
A = [A;Ap1];
B = [B;Bp1];

```

```

% Lower Bounds
LBPdG = zeros(N,1);
LB1k = zeros(SG*N,1);
LBxDG = zeros(N,1);
LBxSU = zeros(N,1);
LBxSD = zeros(N,1);

% NULL lower bounds
LBNULL = zeros(N,1);

% Storage lower bounds
% Your chosen storage initial & final storage states:
LBxb = xbStorageMin.*ones(N,1);
LBxb(1) = xb_measured_state;

LBPb = -Cb.*ones(N,1);
LBdeltb = zeros(N,1);
LBzb = zeros(N,1);

LBPGrid = -Tg*ones(N,1);
LBdeltg = zeros(N,1);
LBCg = -Inf*ones(N,1);
LBZg = 0;

LBBeta_lighting = zeros(161*N,1);

LB = [LBPdG;LB1k;LBxDG;LBxSU;LBxSD;LBNULL;LBxb;LBPb;LBdeltb;LBzb;...
      LBPGrid;LBdeltg;LBCg;LBZg;LBBeta_lighting];

% Upper Bounds
UBPDG = PDG_max.*ones(N,1);
UB1k = Inf.*ones(SG*N,1);
UBxDG = ones(N,1);
UBxSU = ones(N,1);
UBxSD = ones(N,1);

% NULL upper bounds
UBNULL = ones(N,1);

% Storage lower bounds
% Your chosen storage initial & final storage states:
UBxb = xbStorageMax.*ones(N,1);
UBxb(1) = xb_measured_state;

UBPb = Cb.*ones(N,1);
UBdeltb = ones(N,1);
UBzb = Cb*ones(N,1);

UBPGrid = Tg*ones(N,1);
UBdeltg = ones(N,1);

```

```

UBCg = Inf*ones(N,1);

UBZg = Inf;

UBBeta_lighting = ones(161*N,1)*0.15;

UB = [UBPDG;UBlk;UBxDG;UBxSU;UBxSD;UBNULL;UBxb;UBPb;UBdeltb;UBzb;...
      UBPGrid;UBdeltg;UBCg;UBZg;UBBeta_lighting];

intVars = [11*N+1:14*N,17*N+1:18*N,20*N+1:21*N]; % For xDG,xSU,xSD,,deltb,
                                                    % deltg, Beta_plug
ctype = blanks(183*N+1); % Initializing the char array, adding 161
lighting controllable loads
ctype(:) = 'C'; % Set all decision variable as continious. Modify
               % in next line.
ctype(intVars) = 'I'; % set all interger decision variables

xOpt = zeros((183*N+1),1);
[xOpt,fvalILP] = cplexmilp(costs, A, B, Aeq, Beq, [ ], [ ], [ ], LB, UB,...
                        ctype, [ ], [ ]);

%toc

%xOptRound = logical(round(xOpt)); % Rounding all values, if needed
%xOpt = logical(round(xOpt));
xOptRound = round(xOpt); % Removed 'logical' since Simulation error:
                        % 'class mismatch'

% The generation, start,shutoff, storage energy, storage powerflow, and
% grid energy solution values

xPDG = xOpt(1:N); % PDG solution
xLDG = xOpt(N+1:11*N); % LDG solution
xDG = xOptRound(11*N+1:12*N); % xDG solution
xSU = xOptRound(12*N+1:13*N); % start-up solution
xSD = xOptRound(13*N+1:14*N); % shut-down solution
xNULL = xOpt(14*N+1:15*N); % NULL solution
xb = xOpt(15*N+1:16*N); % storage energy solution
xPb = xOpt(16*N+1:17*N); % storage power flow solution
xdeltb = xOptRound(17*N+1:18*N); % delta b solution
xzb = xOpt(18*N+1:19*N); % zb solution
xPgrid = xOpt(19*N+1:20*N); % utility grid Power solution
xdeltg = xOptRound(20*N+1:21*N); % delta g solution
xCg = xOpt(21*N+1:22*N); % Cg solution
xZg = xOpt(22*N+1); % Zg solution
for i=1:161
    xBeta_lighting(i,:)=xOpt((21+i)*N+2:(22+i)*N+1);
end

% The first element of the MILP solution to output

```

```

% These values will be the command values for the microgrid plant
xPDG1 = xPDG(1);
xDG1 = xDG(1);
xSU1 = xSU(1);
xSD1 = xSD(1);
xBeta1 = xBeta(1);
xPb1 = xPb(1);
xdeltb1 = xdeltb(1);
xPgrid1 = xPgrid(1);
xdeltg1 = xdeltg(1);
for i=1:161
xBeta_lighting1(i)=xBeta_lighting(i,1);
end
% for i=1:201
% xBeta_plug1(i)=xBeta_plug(i,1);
% end

lighting_controllable_demand1 = sum((1-
xBeta_lighting1).*light_demand_hat(:,1));
% plug_controllable_demand1 = sum((1-xBeta_plug1).*plug_demand_hat(:,1));

% plug_profile1=zeros(201,1);
light_profile1=zeros(161,1);
% plug_profile1=plug_profile(:,Time_Step);
light_profile1=light_profile(:,Time_Step);
% Plug_penalty =sum(rho_c_plug*(xBeta_plug1).*plug_profile1) ;
Lighting_penalty = sum(rho_c_lighting*(xBeta_lighting1).*light_profile1);

```

APPENDIX B
SIMULINK SIMSCAPE MODEL OF ECS BUILDING MICROGRID AND MPC-
MILP CONTROLLER

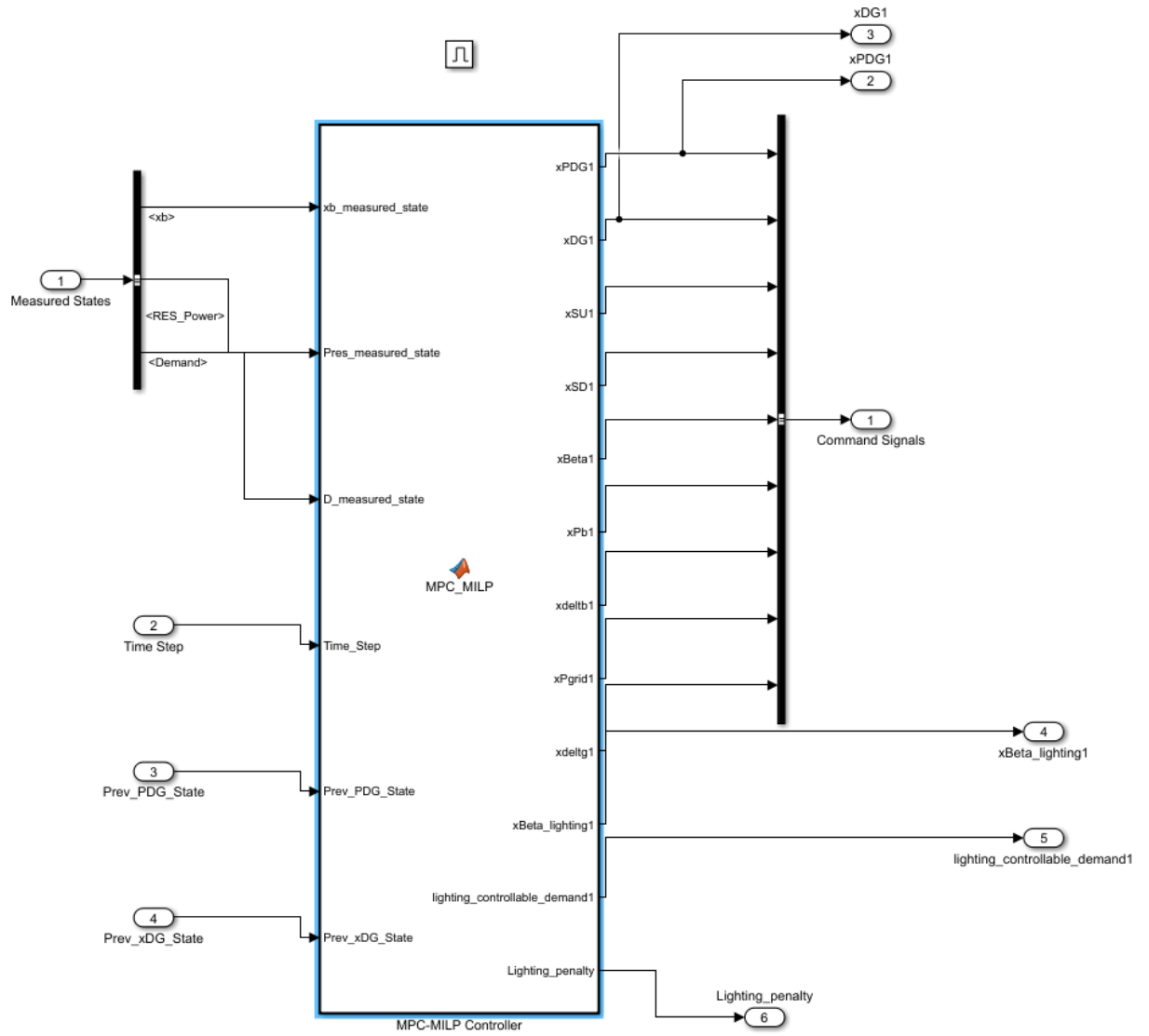


FIGURE: MPC-MILP Controller in Simulink

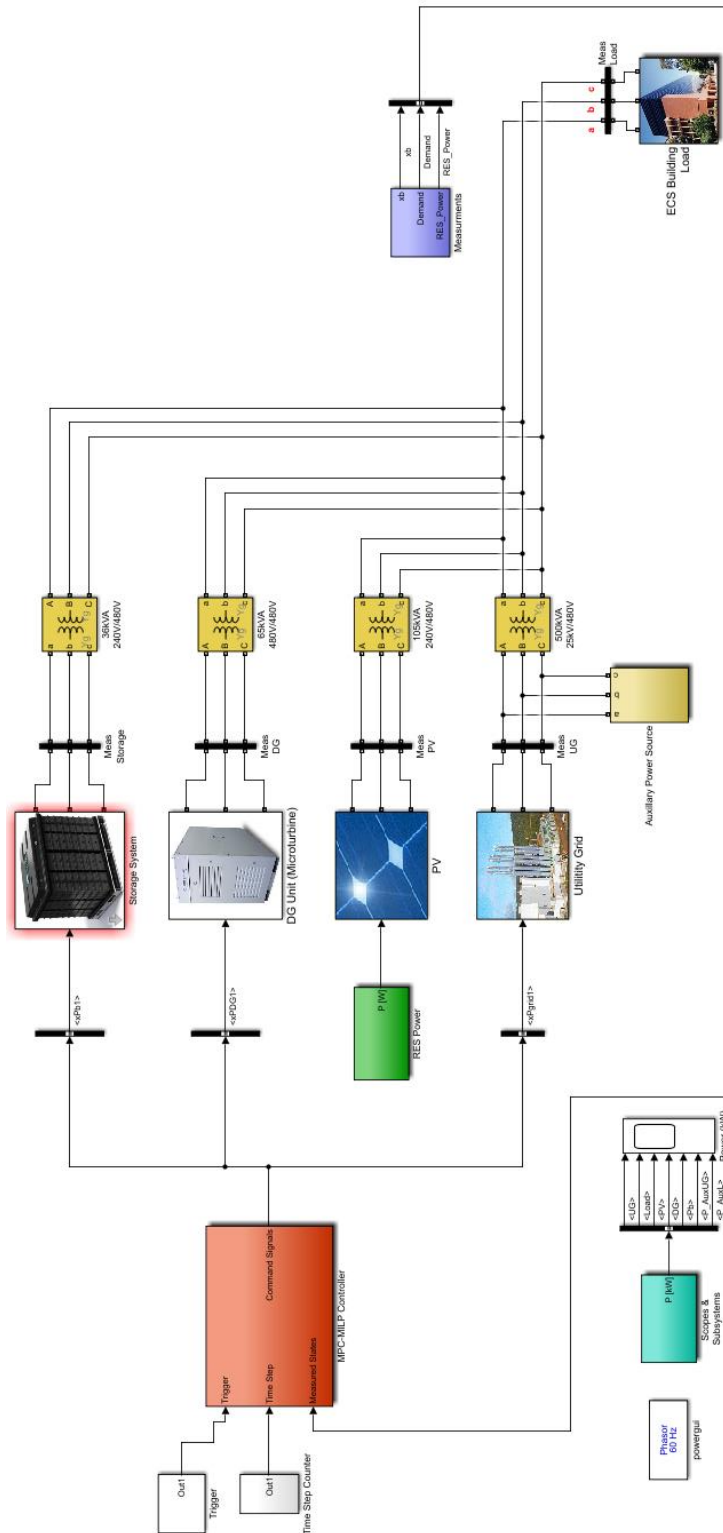


FIGURE: ECS Building Microgrid in Simulink

REFERENCES

REFERENCES

- [1] R. Lasseter and P. Piagi, "Microgrid: A conceptual solution," in Proc. IEEE Annu. Power Elect. Specialists Conf., Jun. 2004, pp. 4285–4290.
- [2] Pacific Northwest GridWise, Testbed demonstration projects. Part II. Grid friendly, Appliance Project, PNNL-17079, Oct. 2007.
- [3] S. Cass, "Big fridge is watching you," IEEE Spectr., vol. 50, no. 6, pp.88–88, 2013.
- [4] T. Bigler, G. Gaderer, P. Loschmidt, and T. Sauter, "Smart Fridge: Demand side management for the device level," in Proc. IEEE 16th Conf. Emerging Technologies and Factory Automation (ETFA), Toulouse, France, Sept. 2011, pp. 1–8.
- [5] M. Botts, G. Percivall, C. Reed, and J. Davidson, OGC sensor web enablement: Overview and high level architecture, in GeoSensor Networks, Lecture Notes in Computer Science, S. Nittel, A. Labrinidis, and A. Stefanidis, Eds. Berlin, Germany: Springer-Verlag, Jan. 2008, vol. 4540, pp. 175190.
- [6] D. Potter, Smart plug and play sensors, IEEE Instrum. Meas. Mag., vol.5, no. 1, pp. 2830, 2002.
- [7] M. Bisadi, A. Akrami, S. Teimourzadeh, F. Aminifar, M. Kargahi and M. Shahidehpour, "IoT-Enabled Humans in the Loop for Energy Management Systems: Promoting Building Occupants' Participation in Optimizing Energy Consumption," in IEEE Electrification Magazine, vol. 6, no. 2, pp. 64-72, June 2018.
- [8] M. Honarvar Nazari and M. Ilic, "Potential for efficiency improvement of future electric energy systems with distributed generation units," IEEE PES General Meeting, Minneapolis, MN, 2010, pp. 1-9.
- [9] M. Manic, D. Wijayasekara, K. Amarasinghe, and J. J. Rodriguez-Andina, "Building energy management systems: The age of intelligent and adaptive buildings," IEEE Ind. Electron. Mag., vol. 10, no. 1, pp. 25–39, 2016.
- [10] F. Katiraei, R. Iravani, N. Hatziargyriou, and A. Dimeas, "Microgrids management," IEEE Power Energy Mag., vol. 6, no. 3, pp. 54–65, May/Jun. 2008.
- [11] M. H. Nazari (2013 Electrical networks of the Azores Archipelago. In: Ilic M., Xie L., Liu Q. (eds) Engineering IT-Enabled Sustainable Electricity Services. Power Electronics and Power Systems, vol 30. Springer, Boston, MA.
- [12] M. H. Nazari, Making the most out of distributed generation without endangering normal operation: A model-based technical-policy approach, 2012.
- [13] D. Mehdi, J. Belhadj, and X. Roboam. "Hybrid solar–wind system with battery storage operating in grid-connected and standalone mode: control and energy management–experimental investigation." Energy 35.6 (2010): 2587-2595.
- [14] W. Ongsakul, N. Petcharak, "Unit commitment by enhanced adaptive Lagrangian relaxation," IEEE Transaction on Power System, 2004.
- [15] T. Logenthiran and D. Srinivasan, "Short term generation scheduling of a MG," in Proc. 2009 IEEE Region 10 Conf. (TENCON), Singapore, pp. 1–6.
- [16] Kuznetsova, Elizaveta, et al. "An integrated framework of agent-based modelling and robust optimization for MG energy management," Applied Energy 129 (2014): 70-88.
- [17] H. A. Ozkan, "A new real time home power management system," Energy and Buildings, vol. 97, pp.56-64, 2015.

- [18] K. M. Tsui and S. C. Chan, "Demand Response Optimization for Smart Home Scheduling Under Real-Time Pricing," *IEEE Transaction on Smart Grid*, vol. 3, no. 4, pp. 1812-1821, 2012.
- [19] Kriett, P.O. and Salani, M. (2012) Optimal Control of a Residential Microgrid. *Energy*, 42, 321-330.
- [20] D. Thomas, O. Deblecker, K. Genikomsakis and C. S. Ioakimidis, "Smart house operation under PV and load demand uncertainty considering EV and storage utilization," *IECON 2017 - 43rd Annual Conference of the IEEE Industrial Electronics Society*, Beijing, 2017, pp. 3644-3649.
- [21] E. Sanchez, and M. H. Nazari, "Model predictive energy scheduling for building microgrid," *2017 North American Power Symposium (NAPS)*, Morgantown, WV, 2017, pp. 1-6.
- [22] A. Parisio, E. Rikos, and L. Glielmo, "A model predictive control approach to microgrid operation optimization," *IEEE Transactions on Control Systems Technology*, 2014.
- [23] U.S. Energy Information Administration, *Annual energy review 2011*, Oct. 2012.
- [24] The United Nations, Environment Programme. [Online]. Available: <http://www.unep.org/sbci/AboutSBCI/Background.asp>
- [25] K. W. Roth, D. Westphalen, M. Y. Feng, P. Llana, and L. Quartararo, *Energy impact of commercial building controls and performance diagnostics: Market characterization, energy impact of building faults and energy savings potential*, TIAX LLC, Cambridge, MA, USA, Tech.Rep.
- [26] A. Chehri and H. T. Mouftah, "Service-oriented architecture for smart building energy management," *2013 IEEE International Conference on Communications (ICC)*, Budapest, pp. 4099-4103, 2013.
- [27] Autodesk Inc. <https://www.autodesk.com/products/revit-family/>
- [28] Enlighted Inc, *Enlighted IoT Applications*, [Online]. Available: <https://www.enlightedinc.com/system-and-solutions/iotapplications>
- [29] *California Building Energy Efficiency Standard, Section 130.1(e) Title 24*, [Online]. Available: <https://www.energy.ca.gov/title24/>
- [30] D. H. Tran, M. H. Nazari, A. Sadeghi-Mobarakeh, and H. Mohsenian- Rad, "Smart Building Design: a Framework for Optimal Placement of Smart Sensors and Actuators," *2019 IEEE PES Innovative Smart Grid Technologies (ISGT)*, Washington, DC, 2019.
- [31] Enlighted Space, [Online]. Available: <https://space.enlightedinc.com/#/login>
- [32] *Enlighted Energy Manager web-based GUI*, [Online]. Available: <https://em-2800-7902.p.enlightedcloud.net/ems/login.jsp>
- [33] L. Wu, "A tighter piecewise linear approximation of quadratic cost curves for unit commitment problems," *IEEE Trans. Power Syst.*, vol. 26, no. 4, pp. 2581–2583, Nov. 2011.
- [34] J. Sumbera, "Modelling generator constraints for the self-scheduling problem", [Online]. Available: <http://energyexemplar.com/wpcontent/uploads/publications/Modellinggenerator-constraints-for-the-self-scheduling-problem-.pdf>
- [35] *Capstone MicroTurbine Model C65 Performance Technical Reference* [Online]. Available: http://www.globalmicroturbine-.com/server/C65/-pages/410048C_C65_Performance_TR.pdf_001.htm

- [36] “Natural Gas Prices,” U.S. Energy Information Administration (EIA). [Online]. Available: <https://www.eia.gov/naturalgas/>.
- [37] E. Sanchez, “A Model Predictive Control Approach to Economic Scheduling for a Building Microgrid (Master’s thesis)” in Electrical and Engineering Department, California State University, Long Beach, May 2018.
- [38] Capstone MicroTurbine Model C65 [Online]. Available: <https://www.capstoneturbine.com/products/c65>
- [39] A. Bemporad and M. Morari, “Control of systems integrating logic, dynamics, and constraints,” *Automatica*, vol. 35, no. 3, pp. 407–427, 1999.
- [40] Aquion Energy Aspen 48M-25.9 AHI Battery Bank [Online]. Available: <https://www.solarelectricsupply.com/aquion-aspen-48m-25-9-ahisaltwater-plug-and-play-battery-bank>
- [41] Rate Schedule TOU-8 - Southern California Edison [Online]. Available: https://www.sce.com/NR/rdonlyres/4393B684-6D2-A-49F0835985DC4CD1D679/0/091022_TOU8_-Fact_Sh...
- [42] “Net Surplus Compensation Rate | Rates & Pricing Choices | SCE Tariff Books | Regulatory Information | Home - SCE,” Southern California Edison. [Online]. Available: <https://www.sce.com/w-ps/portal/home/regulatory/!ut/p/b1/>
- [43] L. Gan, A. Wierman, U. Topcu, N. Chen, and S. H. Low, “Realtime deferrable load control: Handling the uncertainties of renewable generation,” in *Proc. 4th Int. Conf. Future Energy Syst.*, New York, NY, USA, 2013, pp. 113–124 [Online]. Available: <http://doi.acm.org/1-0.1145/2487166.2487179>, ser. e-Energy’13, ACM